nature communications

Article

https://doi.org/10.1038/s41467-024-54347-2

Histamine-tuned subicular circuit mediates alert-driven accelerated locomotion in mice

Received: 30 April 2024

Accepted: 6 November 2024

Published online: 14 November 2024

Check for updates

Lin Yang[1], Mengdi Zhang[1], Yuan Zhou[1], Dongxiao Jiang[1], Lilong Yu[1], Lingyu Xu[1], Fan Fei[1], Wenkai Lin[1], Yanrong Zheng[1], Jiannong Wu[1], Yi Wang[1,2,3] ✉ & Zhong Chen[1,3] ✉

The locomotive action involves diverse coordination, necessitating the integration of multiple motor neural circuits. However, the precise circuitry mechanism governing emotion-driven accelerated locomotion remains predominantly elusive. Here we dissect projections from the tuberomammillary nucleus (TMN) to subiculum (SUB) which promote alert-driven accelerated locomotion. We find that TMN histaminergic neurons respond to high-speed locomotion in both natural and alert acceleration. The TMN-SUB circuit is sufficient but not essential for amplifying accelerated locomotion from low to high-speed movement in basal condition, but it is both sufficient and necessary in alert condition for modulating accelerated locomotion during high-speed escape behavior. TMN histaminergic neuron activates SUB glutamatergic "fast locomotor cell" that projects to retrosplenial granular cortex (RSG) mainly through histamine H2 receptor (H2R). This study reveals the critical role of the histamine-tuned SUB circuit in alert-driven accelerated locomotion in mice, providing a theoretical foundation for comprehending neural circuit mechanisms of instinctive behaviors under alert.

Locomotion constitutes an indispensable facet of daily life and survival in nature. The dynamics of locomotion involve intricate processes such as learning, planning, coordination, and endurance, requiring the orchestration of diverse motor neural circuits and various neurotransmitters signaling[1]. Speed, fluctuating between acceleration and deceleration, is one of the important characteristics of locomotion execution, embodying both low-speed exploration and high-speed escape[2]. Active accelerated locomotion symbolizes the sensitivity of animals to environmental changes and adaptive capabilities in facing survival challenges to gain an advantage in the intense competition for survival[3]. Plenty of behaviors including powerful desire to find mates or to escape, in response to the emotional innate of hunger or fear, were reflected by accelerated locomotion[4]. However, the intricate circuitry-level mechanism governing emotion-driven accelerated locomotion in the brain remains largely undisclosed. Histaminergic neurons in the tuberomammillary nucleus (TMN) provide the histamine across the whole brain by its wide fiber projections[5]. As one kind of monoamine neurotransmitter in the brain, neuronal histamine synthesized in the histaminergic neurons in the TMN modulates various behavioral states[6,7]. Considering the widely spatial distribution of the histaminergic fibers, aligned with the localization of histamine receptor, which makes the TMN histaminergic system as an important and complicated role in various physiological behaviors[6,8–10]. Alert, as an innate state in animal, ensures adaptive responses to circumstances. As the potential alert signal in the brain[11,12], central histaminergic signaling ensures adaptive responses in the recognition of the danger sense or threat circumstances. Although histamine's involvement in spontaneous locomotion is acknowledged, it remains a subject of

[1]Key Laboratory of Neuropharmacology and Translational Medicine of Zhejiang Province, School of Pharmaceutical Sciences, The First Affiliated Hospital of Zhejiang Chinese Medical University (Zhejiang Provincial Hospital of Chinese Medicine), Zhejiang Chinese Medical University, Hangzhou, Zhejiang, PR China. [2]Zhejiang Rehabilitation Medical Center Department, The Third Affiliated Hospital of Zhejiang Chinese Medical University, Hangzhou, Zhejiang, PR China. [3]Institute of Pharmacology and Toxicology, College of Pharmaceutical Sciences, Zhejiang University, Hangzhou, Zhejiang, PR China.
✉e-mail: wang-yi@zju.edu.cn; chenzhong@zju.edu.cn

controversy due to the complexity of neural circuits and neuronal types[10,13–17]. Yet, little is known about the histaminergic mechanism at circuitry level in emotion-driven accelerated locomotion. In this study, we identify the role of histaminergic neurons in general accelerated locomotion, especially under alert condition, delineating the subiculum (SUB)-projecting histaminergic circuit and cellular mechanism. We unveil that TMN-SUB histaminergic circuit encodes the accelerated locomotion by activating retrosplenial granular cortex (RSG)-projecting SUB glutamatergic "fast locomotor cell" via histamine H2 receptor (H2R). Our finding establishes a theoretical foundation for understanding how neural circuit mechanisms operate alert-driven accelerated locomotion.

Results

TMN histaminergic neurons dynamically response to general accelerated locomotion

To examine the response of TMN histaminergic neurons during locomotion, we quantified the locomotion-induced c-fos expression-a marker utilized for quantifying the neuronal response to stimuli[18], in *HDC-CreERT2: Ai47* hybrid mice. The *HDC-CreERT2: Ai47* hybrid mice were characterized by high efficiency and specificity to label TMN histaminergic neurons (Fig. 1a), and we found that TMN histaminergic neurons were activated by treadmill locomotion training (Fig. 1b). To dynamically investigate the neuronal response during different phase of locomotion in a real-time manner, we performed in vivo fiber photometry recording by expressing the GCaMP6m on TMN histaminergic neurons in *HDC-CreERT2* mice (Fig. 1c). We monitored the calcium activity of TMN histaminergic neurons of freely moving mice in the open field test, and found that TMN histaminergic neurons showed a substantially increased activity when the mice during accelerated locomotion as the movement speed increased (Fig. 1d1). To dissect the TMN histaminergic neurons activity in the accelerated locomotion, we analyzed the initiation of the accelerated locomotion, revealing an increased calcium activity of TMN histaminergic neurons (Fig. 1d2). Rotarod test, serving as a reflection of animal locomotion balance and accelerated locomotion, demonstrated an initial increase in TMN histaminergic neurons activity at the onset of the test. However, there was no subsequent increase as the rotarod speed accelerated (Fig. 1e, f). Subsequently, we addressed whether TMN histaminergic neuronal activity responds changes in locomotion speed using the treadmill test that included both acceleration and deceleration states (Fig. 1g). Notably, TMN histaminergic neurons activity increased during the acceleration period, remaining unaffected during decelerated locomotion (Fig. 1h, i). These findings suggest TMN histaminergic neuronal activity specifically responds to general accelerated locomotion.

In nature, the law of survival of the fittest prompted many animals to develop a keen sense of alertness, enabling swift recognition of threats and rapid action of escape. Importantly, histamine plays a critical role in regulating the sleep-wake rhythm and attention behaviors, which was considered as a potential alert signal in the brain[11,12]. Both the freely movement and escape behavior are considered as active locomotion process[19,20], and accelerated locomotion as a key initiation factor that largely determined the escape ability of animal[21]. We thus hypothesized that the TMN histaminergic neurons might play a role in the context of accelerated alert-escape behavior. To address that, we monitored the activity of TMN histaminergic neurons during various alert behaviors (Supplementary Fig. 1a, b). We found that an increase in calcium activity of TMN histaminergic neurons was observed during rearing (Supplementary Fig. 1c–e), an innate alert behavior during exploration[22,23]. We then subjected mice to two other behaviors associated with higher threat levels: novel object approaching and water spray test. Novel object approaching involves visual exploration, while back water spray elicited alert behavior in response to somatosensory sources, both of which are danger signals that evoke alertness[24]. The activity of TMN histaminergic neurons increased when faced with an approaching unfamiliar object (Supplementary Fig. 1f–h) or after water spray (Supplementary Fig. 1i–k). These data suggest that the activity of TMN histaminergic neurons is in response to distinct alert behaviors. Escape behavior, characterized by accelerated running or jumping away from the perceived threat usually occurs in a state of heightened alert[25,26]. To simulate the alert induced escape behavior induced by mice facing natural enemies or intruders in nature, social attack-escape test was used in our study. We recorded the changes in calcium activity of TMN histaminergic neurons during the alert-escape behavior, and found that calcium fluorescence signals were rapidly increased as mice exhibited higher acceleration, remaining elevated level even after locomotion speed returned to baseline (Fig. 1j, k). This suggests that TMN histaminergic neurons are strongly activated during alert-related emotional responses. These results demonstrate that TMN histaminergic neuronal activity specifically responds to accelerated locomotion in both neutral and alert conditions.

TMN histaminergic neurons modulate accelerated locomotion in heightened alert condition

To elucidate the causal role of TMN histaminergic neurons in accelerated locomotion, we employed the optogenetic approach to activate the TMN histaminergic neurons by infusion of the AAV-CAG-FLEX-oChIEF-tdTomato into the TMN of *HDC-CreERT2* mice and the immunofluorescence results confirmed that the oChIEF was strictly expressed on TMN histaminergic neurons (Supplementary Fig. 2a). Out of expectation, optogenetic activation of TMN histaminergic neurons demonstrated no apparent effect on the distance or speed of active spontaneous locomotion in mice under neutral condition (Supplementary Fig. 2b–e). Similarly, optogenetic inhibition of TMN histaminergic neurons, achieved by expressing the opsin archaerhodopsin (AAV-CAG-FLEX-ArchT-GFP), had no influence on spontaneous locomotion in mice in neutral condition (Supplementary Fig. 2f–j).

Then, we proceeded to investigate whether manipulation of TMN histaminergic neurons would affect alert-escape behavior via optogenetic approaches. Surprisingly, optogenetic activation of TMN histaminergic neurons increased the distance, especially escape average speed, and escape max speed (Supplementary Fig. 1l–n), suggesting the role of promoting accelerated locomotion of TMN histaminergic neurons in heightened alert condition. In contrast, optogenetic inactivation of TMN histaminergic neurons led to a decrease in distance, escape average speed, and escape max speed (Supplementary Fig. 1o–q). These results indicate that TMN histaminergic neurons modulate accelerated locomotion that is context dependent, especially under heightened alert condition, like alert-escape behavior.

TMN-SUB histaminergic circuit promotes accelerated locomotion

Then we investigated how TMN histaminergic neurons route accelerated information in circuitry level. In vertebrate animals, locomotion originates from the mesencephalic locomotor command center and is subsequently mediated by the lateral gigantocellular reticulospinal system, where receive input from many brain regions including the basal ganglia[27,28]. Of noted, speed cells encoding speed information were identified mainly in entorhinal cortex (EC)[29]. Additionally, SUB serves as the output of the hippocampus complex, encoding speed, location, and trajectory trace information[30], with angular speed cell and linear speed cell distributed in para-SUB and pre-SUB[31]. Importantly, our lab's previous whole brain TMN histaminergic neurons mapping revealed the distribution of TMN histaminergic fibers in SUB and EC[5]. To further address whether SUB or EC involves in the locomotion function of histaminergic system, we injected the histamine sensor (AAV-hSyn-HA1h), capable of dynamically monitoring histamine concentration changes[8,12], into SUB (Fig. 2a) and EC (Fig. 2c) to elucidate the histamine level in different locomotion phases. Initially,

https://doi.org/10.1038/s41467-024-54347-2

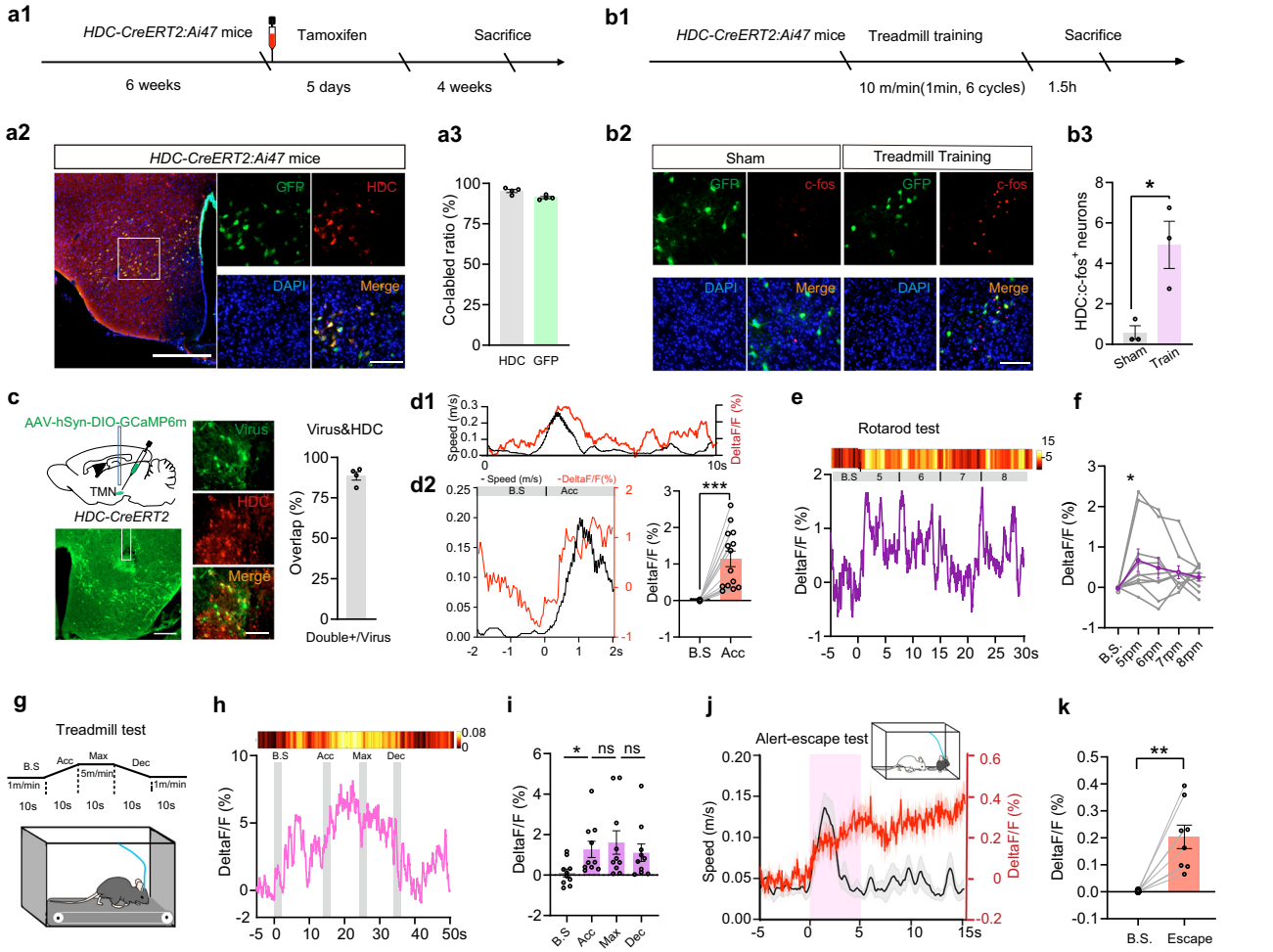

Fig. 1 | Accelerated locomotion increases the calcium activity of TMN histaminergic neurons. a Experimental timeline (**a1**), representative images (**a2**), and validation (**a3**) of the *HDC-CreERT2: Ai47* mice. Scale bar = 400 μm, $n = 4$ mice; Enlarged image, scale bar = 100 μm. **b** Schematic timeline (**b1**), representative images (**b2**), and quantification of c-fos activation in TMN (**b3**) of locomotion training mice, scale bar = 100 μm, $n = 3$ mice, $^{*}p = 0.0233$. **c** Schematic, representative images and quantification of viral expression in the TMN in *HDC-CreERT2* mice transfected with AAV-hSyn-DIO-GCaMP6m, $n = 4$ mice (left, scale bar = 100 μm; right, scale bar = 50 μm). **d1** Representative speed (black) and corresponding calcium activity (red) of TMN histaminergic neurons of *HDC-CreERT2* mice during locomotion in the open field test. **d2** Representative fluorescence signal of calcium activity with corresponding speed, and quantification of calcium activity of TMN histaminergic neurons during locomotor acceleration (Acc). $n = 14$ mice, $^{***}p = 0.0001$ vs. baseline (B.S). Representative fluorescence signal and heatmap (**e**), and quantification of calcium activity (**f**) of TMN histaminergic neurons in the rotarod test. $n = 10$ mice, $^{*}p = 0.0431$ B.S vs. 5 rpm, $p = 0.1956$ B.S vs. 6 rpm, $p = 0.3866$ B.S vs. 7 rpm, $p = 0.7024$ B.S vs. 8 rpm. Schematic diagram (**g**), fluorescence value and heatmap (**h**), and quantification of calcium activity (**i**) of TMN histaminergic neurons during B.S, Acc, max speed (Max), and deceleration (Dec) period in the treadmill test ($n = 10$ mice, $^{*}p = 0.0125$ Acc vs. B.S, $p = 0.3485$ Max vs. Acc, $p = 0.1041$ Dec vs. Max; ns non-significant). Fluorescence values with corresponding speed (**j**), and quantification of calcium activity (**k**) of TMN histaminergic neurons during alert-escape test. $n = 8$ mice, $^{**}p = 0.0022$. Two-tailed Student's *t* test for (**b3**, **d2**, **i**, **k**) and one-way ANOVA followed by the Dunnett post hoc test for (**f**). Schematics in **a1**, **b1**, **c**, **g**, **j** were drew by PowerPoint. Bar graphs represent mean ± SEM. Source data are provided as a Source Data file.

we monitored the histamine concentration changes in SUB of freely moving mice during the open field test, revealing an increase in histamine concentration during accelerated locomotion as the mice's movement speed increased (Fig. 2b). Conversely, histamine level exhibited variable changes in EC (Fig. 2d). Similarly, we analyzed the initiation of the acceleration, observing an increased level of histamine concentration in SUB (Fig. 2e, f), but not in EC (Fig. 2g, h). Crucially, histamine signal in SUB gradually increased during the rotarod test as rotarod speed accelerated (Fig. 2i, j), whereas in EC, it displayed a fluctuating pattern (Fig. 2k, l). Notably, the histamine concentration level in SUB specifically increased at the accelerated locomotion period in the treadmill test (Fig. 2m, n), and this phenomenon was not observed in EC (Fig. 2o, p). The above recordings in EC appeared to be quite noisy, which could be due to several factors. The EC is a large brain region that can be divided into lateral and medial EC along the medial-lateral axis, and into superficial and deep layer from top to bottom[32,33]. Importantly, the EC has a highly complex cellular composition, including functionally distinct cell types such as grid cells, head direction cells, speed cells, border cells, and object-vector cells[34,35]. This complexity may contribute to the variability in fluorescence signal recordings of histamine in the EC. Importantly, we also detected an elevation in histamine concentration level in SUB during rearing, novel object approaching, and water spray, as well as accelerated locomotion during alert-escape behavior (Supplementary Fig. 3). These results suggest that histamine concentration level in SUB but not EC specifically coupled with accelerated locomotion in both neutral and alert conditions.

To probe the functional engagement of TMN-SUB histaminergic circuit in accelerated locomotion, we injected the TMN with AAV-hSyn-FLEX-ChrimsonR-tdTomato in *HDC-CreERT2* mice and histamine sensor in SUB (Supplementary Fig. 4a). Utilizing fiber photometry recording, we found an elevation in histamine concentration in SUB

https://doi.org/10.1038/s41467-024-54347-2

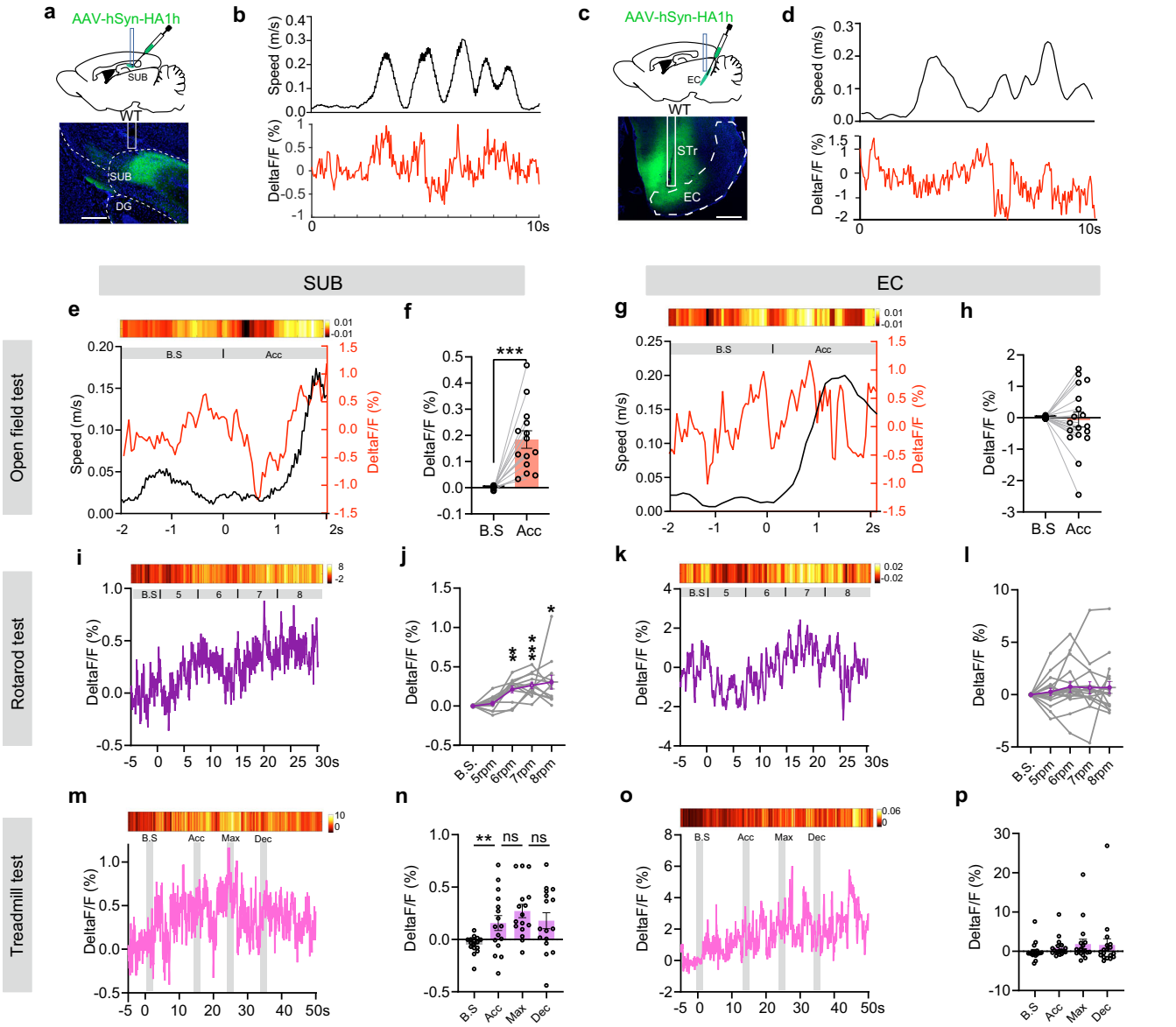

Fig. 2 | Accelerated locomotion increases histamine release in the SUB but not EC. Schematic diagram and representative image of viral injection of AAV-hSyn-HA1h into the SUB (**a**) or EC (**c**) of WT mice. Scale bar = 200 μm. The representative speed (upper) and corresponding fluorescence signal of histamine concentration changes (bottom) in SUB (**b**) or EC (**d**) during locomotion in the open field test. Fluorescence signal, heatmap, corresponding speed, and quantification of the mean fluorescence values of histamine concentration changes in SUB (**e**, **f**) or EC (**g**, **h**) during locomotor acceleration. $n = 14$ mice, $^{***}p = 0.0001$ for (**f**), $n = 18$ mice, $p = 0.7850$ for (**h**). Representative fluorescence signal, heatmaps, and quantification of mean fluorescence values of histamine concentration changes in SUB (**i**, **j**) or EC (**k**, **l**) during the rotarod test (**j**: $n = 12$ mice, $p = 0.5537$ B.S vs. 5 rpm, $^{**}p = 0.0016$ B.S vs. 6 rpm, $^{***}p = 0.0002$ B.S vs. 7 rpm, $^{*}p = 0.0187$ B.S vs. 8 rpm; **l**: $n = 18$ mice, $p = 0.8322$ B.S vs. 5 rpm, $p = 0.4192$ B.S vs. 6 rpm, $p = 0.6334$ B.S vs. 7 rpm, $p = 0.5721$ B.S vs. 8 rpm). Representative fluorescence signal, heatmap, and quantification of mean fluorescence values of histamine concentration changes in SUB (**m**, **n**) or EC (**o**, **p**) during treadmill test (**n**: $n = 16$ mice, $^{**}p = 0.0046$ Acc vs. B.S, $p = 0.0720$ Max vs. Acc, $p = 0.0855$ Dec vs. Max; **p**: $n = 18$ mice, $p = 0.2022$ Acc vs. B.S, $p = 0.1775$ Max vs. Acc, $p = 0.6324$ Dec vs. Max). Two-tailed Student's t test for (**f**, **h**, **n**, **p**) and one-way ANOVA followed by the Dunnett post hoc test for (**j**, **l**). Schematics in **a**, **c** were drew by PowerPoint. Bar graphs represent mean ± SEM. Source data are provided as a Source Data file.

during photo-stimulation of TMN-SUB terminals (Supplementary Fig. 4b–d), suggesting the functional activation of histaminergic fibers terminals in SUB. To rule out the effect of excitation lights on the signal of histamine, we conducted a control experiment by infusing AAV-CAG-DIO-mCherry and histamine sensor into TMN and SUB respectively in *HDC-CreERT2* mice, and the data indicated that photo-stimulation of TMN-SUB terminals did not affect the histamine sensor signal in SUB (Supplementary Fig. 4e–h).

Then, we found that the mice exhibited a transient increase in speed when activated TMN-SUB circuit terminals (Fig. 3a, b), indicating the potential promoting accelerated locomotion of this histaminergic circuit. To validate the hypothesis, locomotion index of freely movement was analyzed, and found that activation of TMN-SUB circuit resulted in an overall increase in the total distance traveled in the open field (Fig. 3c–e). To better characterize the pro-locomotion effects of activation of TMN-SUB histaminergic circuit, we categorized the speed of mice based on previous studies[2,36], and combined with the average and max speed of mice observed in the open field test: super low-speed (0–0.01 m/s), low speed (0.01–0.02 m/s), intermediate speed (0.02–0.05 m/s), high-speed (0.05–0.1 m/s) and super high-speed (0.1–0.5 m/s). Interestingly, photo-stimulation led to a decrease in time spent in super low-speed locomotion whereas increasing the time

https://doi.org/10.1038/s41467-024-54347-2

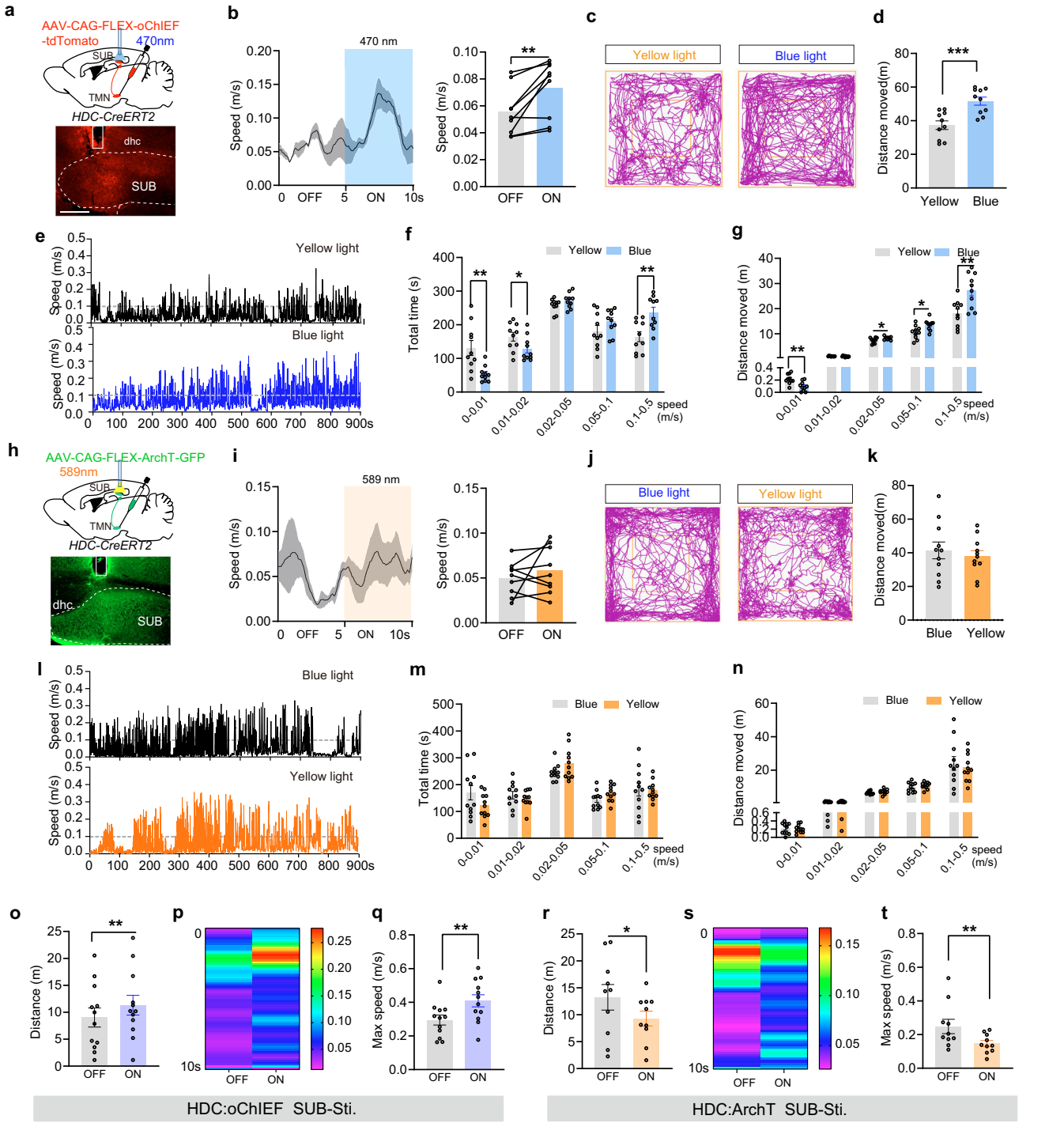

Fig. 3 | TMN-SUB histaminergic circuit bidirectionally regulates accelerated locomotion in alert condition. a Schematic of injection of AAV-CAG-FLEX-oChIEF-tdTomato into the TMN of *HDC-CreERT2* mice (top), and optic fiber position in SUB (bottom), scale bar = 100 μm. **b** Representative velocity curve and speed upon TMN-SUB circuit activation in open field test. $n = 9$ mice, $^{**}p = 0.0086$. Representative traveled tracks (**c**), distance (**d**), representative velocity distribution (**e**), and 5-speed subsections analysis for active time (**f**), distance (**g**) of *HDC-CreERT2: oChIEF* mice, $n = 10$ mice (**d**: $^{***}p = 0.0007$; **f**: $^{**}p = 0.0036$, $^{*}p = 0.0471$, $p = 0.1720$, $p = 0.1763$, $^{**}p = 0.0030$; **g**: $^{**}p = 0.0026$, $p = 0.3348$, $^{*}p = 0.0296$, $^{*}p = 0.0116$, $^{**}p = 0.0040$). **h** Schematic of injection of AAV-CAG-FLEX-ArchT-GFP into the TMN of *HDC-CreERT2* mice (top), and optic fiber position in SUB (bottom), scale bar = 100 μm. **i** Representative velocity curve and speed upon TMN-SUB circuit inhibition in open field test. $n = 9$, $p = 0.3502$. Representative traveled tracks (**j**), distance (**k**), velocity distribution (**l**), and 5-speed subsections analysis for active time (**m**), distance (**n**) of *HDC-CreERT2: ArchT* mice, $n = 11$ mice (**k**: $p = 0.5722$; **m**: $p = 0.1325$, $p = 0.4365$, $p = 0.1211$, $p = 0.0811$, $p = 0.8820$; **n**: $p = 0.8981$, $p = 0.6708$, $p = 0.2177$, $p = 0.4035$, $p = 0.6132$). Effects of optogenetic activation of TMN-SUB terminals on distance (**o**), average speed heatmap (**p**), and max escape speed (**q**) of *HDC-CreERT2: oChIEF* mice during alert-escape test. $n = 12$ mice (**o**: $^{**}p = 0.0044$; **q**: $^{**}p = 0.0063$). Effects of optogenetic inhibition of TMN-SUB terminals on distance (**r**), average speed heatmap (**s**), and max escape speed (**t**) of *HDC-CreERT2: ArchT* mice during alert-escape test. $n = 10$ mice (**r**: $^{*}p = 0.0176$; **t**: $^{**}p = 0.0073$). Two-tailed Student's *t* test for (**b**, **d**, **f**, **g**, **i**, **k**, **m**–**o**, **q**, **r**, **t**). Schematics in **a**, **h** were drew by PowerPoint. Bar graphs represent mean ± SEM. Source data are provided as a Source Data file.

spent in super high-speed locomotion (Fig. 3f). Analyzing the traveled distance in each speed subsection, we found that the locomotion-promoting effect of the TMN-SUB circuit activation was driven by enhancing super high-speed and high-speed locomotion, as well as reducing super low-speed locomotion (Fig. 3g). To test the sufficiency of TMN-SUB histaminergic circuit in promoting accelerated locomotion under alert condition, optogenetic gain of function was performed and the data showed that activation of TMN-SUB histaminergic terminals increased the distance and escape max speed in alerts-escape behavior (Fig. 3o–q). These data suggest that optogenetic activation of TMN-SUB histaminergic circuits enhances accelerated locomotion from low-speed to high-speed movement in both neutral and alert conditions.

We next explored the necessity of the TMN-SUB histaminergic circuit in accelerated locomotion by optogenetic inhibition of the TMN-SUB circuit (Fig. 3h). Contrary to expectation, photo-inhibition of TMN-SUB histaminergic circuit showed no effects on locomotion in neutral conditions (Fig. 3i–n). This could be attributed to the relatively low histamine activity in neutral condition. While, in alert conditions, optogenetic inactivation of the TMN-SUB histaminergic circuit decreased the distance and escape max speed in alerts-escape behavior (Fig. 3r–t). For comparative purpose, we endeavored to manipulate the TMN-EC histaminergic circuit in locomotion by implanting the optic fiber above EC. We found that optogenetic modulation (either activation or inhibition) of the TMN-EC histaminergic circuit exhibited no discernible effect on locomotion (Supplementary Fig. 5). All above data suggest that while the TMN-SUB histaminergic circuit is sufficient, but not necessary, to promote accelerated locomotion in neutral condition; while in alert conditions TMN-SUB histaminergic circuit is both sufficient and necessary to modulate accelerated locomotion.

SUB glutamatergic neurons mediate the pro-locomotion function of the TMN-SUB histaminergic circuit

Next, we delved into investigating the downstream cellular type in the SUB, which includes major long-projecting excitatory glutamatergic neurons and minor local inhibitory GABAergic neurons[37–39]. Employing an activity-dependent neural tagging approach with the ESARE promoter (Enhanced Synaptic Activity-Responsive Element)[40,41], we labeled the cells in the SUB response to photoactivation of TMN-SUB circuits by injected the photo-activation virus (AAV-CAG-FLEX-oChIEF-tdTomato) into TMN and tamoxifen-induced expression of mixed AAV-EF1a-DIO-EYFP and AAV-ESARE-ERT2-Cre-ERT2 into SUB in *HDC-CreERT2* mice (TMN-SUB sti. activated, Fig. 4a). Subsequent staining data revealed that 86.5% of TMN-SUB activated SUB neurons overlapped with CaMKIIα (glutamatergic neuron maker), without overlapping with GABAergic neuron marker (Fig. 4b). To ascertain whether TMN histaminergic neurons directly project to SUB glutamatergic neurons, we used the monosynaptic rabies viral tracing system (Fig. 4c). Examination of brain slices containing RV indicated that TMN regions could be traced by RV, overlapping with HDC^+ (Fig. 4d). Moreover, we found optogenetic activation of TMN-SUB terminals directly increased the activity of SUB glutamatergic neurons (Fig. 4e–h). As a comparison, photo-stimulation of TMN-SUB terminals in the control virus group (AAV-CAG-DIO-mCherry) did not affect the activity of SUB glutamatergic neurons (Supplementary Fig. 6). These results provide evidence that TMN histaminergic neurons directly project to and functionally activate SUB glutamatergic neurons.

We then detected whether the calcium activity of SUB glutamatergic neurons is associated to accelerated locomotion by injecting the SUB with AAV-CaMKIIα-GCaMP6s (Fig. 4i, j). The fiber photometry revealed that SUB glutamatergic neurons exhibited increased activity in correlation with accelerated locomotion, particularly during the initiation of acceleration in the open field test (Fig. 4k), and rotarod test (Fig. 4l, m). In line with the characteristics of speed cell[29], interestingly, we found that SUB glutamatergic neuron activity increased during accelerated locomotion period compared to baseline, and decreased in the decelerated locomotion compared with the max speed locomotion period in the treadmill test (Fig. 4n, o). Of noted, alert behaviors activated SUB glutamatergic neurons (Supplementary Fig. 7), especially in the accelerated locomotion during alert-escape behavior (Fig. 4p, q). These findings suggest that SUB glutamatergic neurons dynamically respond to speed of locomotion.

We next tested the chemogenetic gain of function of SUB glutamatergic neurons in locomotion by expressing hM3D under the control of CaMKIIα promoter in SUB (Fig. 5a). We verified that an intraperitoneal injection of clozapine-N-oxide (CNO) excited most of hM3D-infetced neurons (Fig. 5b). As expected, chemogenetic activation of SUB glutamatergic neurons increased the total distance and average speed of mice (Fig. 5c, d), indicated by enhancing the high-speed and super high-speed locomotion while decreasing the proportion of super low-speed and low-speed locomotion (Fig. 5e–g). To determine whether SUB glutamatergic neurons mediate the promotion of accelerated locomotion of the TMN-SUB histaminergic circuit, we concurrently stimulated the TMN-SUB histaminergic circuit and inhibited SUB glutamatergic neurons in the same mice (Fig. 5h). Interestingly, the chemogenetic inactivation of SUB glutamatergic neurons alone had a tendency of slightly inhibitory effect on locomotion, but it effectively blocked the promotion effect of accelerated locomotion induced by photo-stimulation of TMN-SUB histaminergic circuit (Fig. 5i, j). Collectively, these converging lines of evidence indicate that SUB glutamatergic neurons serve as the downstream effector of TMN-SUB histaminergic circuit driving accelerated locomotion.

H2R in SUB glutamatergic neurons mainly mediates the pro-locomotion function of the TMN-SUB histaminergic circuit

Three types of histamine receptors (histamine H1/H2/H3 receptors, H1R/H2R/H3R) belonging to G protein-coupled receptors that have been identified in the brain especially in the hippocampus[42,43]: Among these, H1R and H2R are situated at postsynaptic sites mediate most action of histamine in the brain in terms of regulating neural excitability[44], while H3R is found in both pre- and postsynaptic membranes[45]. The H3R is primarily expressed in presynaptic location, which mainly involves in the presynaptic inhibition of histamine or other neurotransmitters release in the brain[46]. To test the involvement of histamine receptors in locomotion modulation, we implanted a cannula into SUB for the administration of the H3R antagonist-thioperamide (Thio). Consistent with the photoactivation of the TMN-SUB histaminergic circuit, intra-SUB administration of Thio increased the locomotion of mice (Fig. 6a–c), by increasing the super low-speed and low-speed locomotion into super high-speed locomotion (Fig. 6d, e). Importantly, we injected a genetically engineered caspase-3 to specifically ablate TMN histaminergic neurons and fibers by infusing the AAV-EF1a-FLEX-taCasp3-TEVp into the TMN of *HDC-CreERT2* mice (Supplementary Fig. 8a). The immunofluorescence data showed that 89.5% of HDC^+ neurons were lost after expression of AAV-EF1a-FLEX-taCasp3-TEVp compared with control group (Supplementary Fig. 8b). In this condition, we found that the pro-locomotion effect of intra-SUB delivery of Thio was abolished in the *HDC-CreERT2:taCasp3* mice (Supplementary Fig. 8c, d). These results support that pro-locomotion effect of Thio in the SUB depends on the presynaptic action of H3R.

Further, we found that H1R agonist, 2-(2-pyridyl)-ethylamine (2-Pel) or H2R agonist, amthamine (Amt) could replicate the pro-locomotion effect of Thio (Fig. 6e, f). To address whether H1R or H2R is necessary to the pro-locomotion effect of Thio, we used H1R/H2R related antagonist. The action of Thio was blocked after pretreatment of H2R antagonist (zolantidine, Zol) along with its downstream targets in regulation of neural excitability: adenine cyclase inhibitor (SQ 22536)[47], and HCN

https://doi.org/10.1038/s41467-024-54347-2

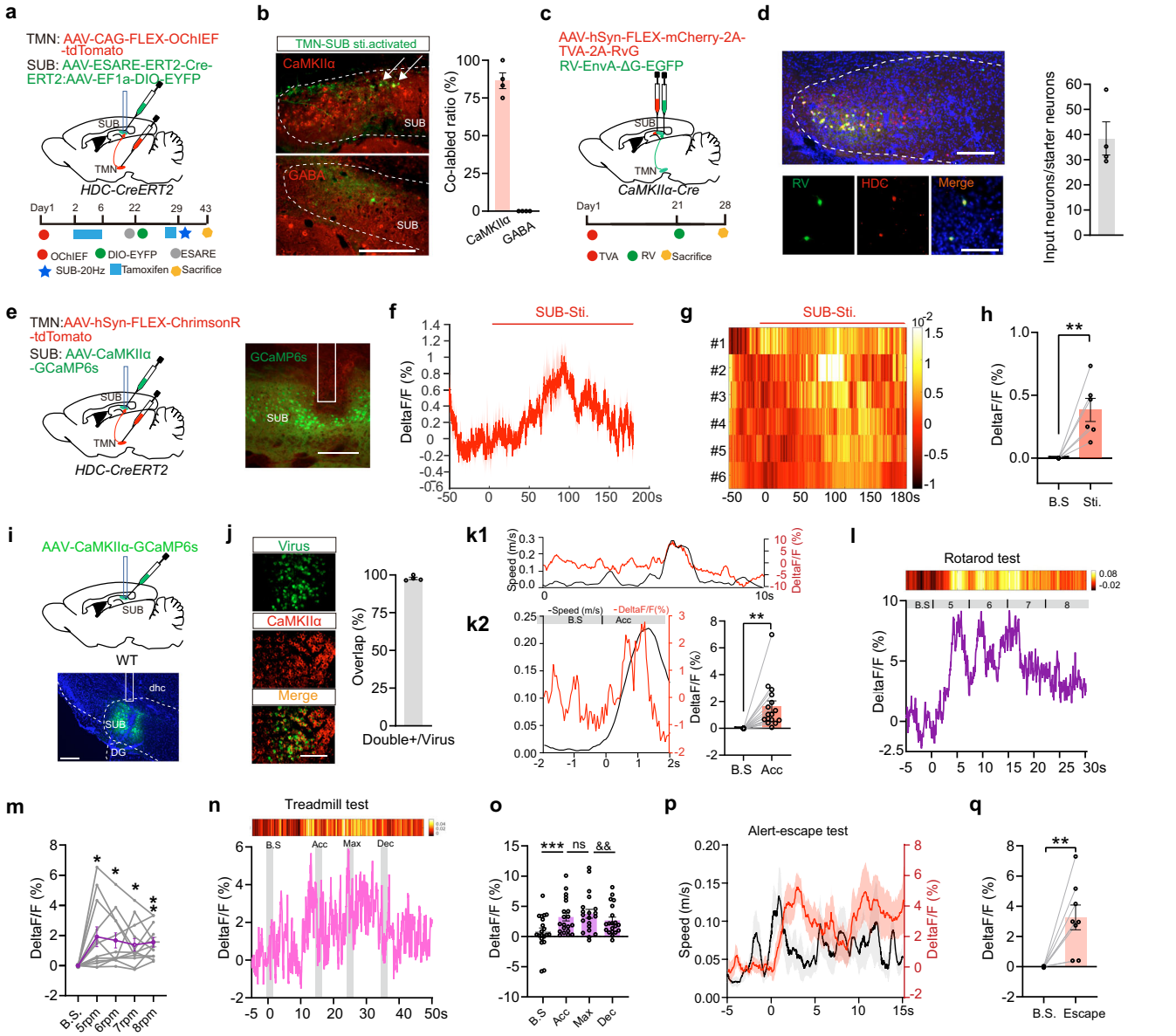

Fig. 4 | SUB glutamatergic neuron is the downstream target of the TMN-SUB histaminergic circuit. *HDC-CreERT2* mice were injected with AAV-CAG-FLEX-oChIEF-tdTomato into TMN and mixed AAV-EF1a-DIO-EYFP, AAV-ESARE-ERT2-Cre-ERT2 to label TMN-SUB activated c-fos+ neurons (TMN-SUB sti. activated) in SUB (**a**), and immunostaining of CaMKIIα/GABA (**b**), scale bar = 200 μm, $n = 4$ mice. **c**, **d** *CaMKIIα-Cre* mice were injected with AAV-hSyn-FLEX-mCherry-2A-TVA-2A-RvG and RV-EnvA-△G-EGFP into SUB, with starter cells in SUB (top, scale bar = 200 μm), SUB-projecting TMN neurons (bottom, scale bar = 100 μm), and quantification, $n = 4$ mice. **e** *HDC-CreERT2* mice were injected with AAV-hSyn-FLEX-ChrimsonR-tdTomato into TMN and AAV-CaMKIIα-GCaMP6s into SUB, scale bar = 100 μm. Fluorescence values (**f**), heatmaps (**g**) and quantification (**h**) of calcium activity during TMN-SUB circuit activation. $n = 6$ mice, $^{**}p = 0.0087$. **i** WT mice were injected with AAV-CaMKIIα-GCaMP6s into SUB, scale bar = 200 μm. **j** Images and quantification of CaMKIIα staining, scale bar = 50 μm, $n = 4$ mice. **k** Representative speed and corresponding calcium activity during locomotion (**k1**), acceleration (**k2**, left), and quantification (**k2**, right) of SUB glutamatergic neuronal activity. $n = 16$ mice, $^{**}p = 0.0017$. Fluorescence signal, heatmaps (**l**), and quantification (**m**) of SUB glutamatergic neuronal activity during rotarod test. $n = 12$ mice, $^{*}p = 0.0432$ B.S vs. 5 rpm, $^{*}p = 0.0205$ B.S vs. 6 rpm, $^{*}p = 0.0229$ B.S vs. 7 rpm, $^{**}p = 0.0017$ B.S vs. 8 rpm. Fluorescence signal, heatmaps (**n**), and quantification (**o**) of SUB glutamatergic neuronal activity during treadmill test. $n = 20$ mice, $^{***}p = 0.0003$ Acc vs. B.S, $p = 0.4823$ Max vs. Acc, $^{\&\&}p = 0.0028$ Dec vs. Max. Speed, fluorescence values (**p**), and quantification (**q**) of SUB glutamatergic neuronal activity during alert-escape test. $n = 8$ mice, $^{**}p = 0.0051$. Two-tailed Student's *t* test for (**h**, **k2**, **o**, **q**) and one-way ANOVA followed by the Dunnett post hoc test for (**m**). Schematics in **a**, **c**, **e**, **i** were drew by PowerPoint. Bar graphs represent mean ± SEM. Source data are provided as a Source Data file.

channel blocker (ZD 7288)[9]. Conversely, pretreatment of H1R antagonist (pyrilamine, Pyr) and its downstream phospholipase C inhibitor (U-73122)[47] showed no statistically significant effect on (although there was a tendency to block) the action of Thio (Fig. 6h, i).

As drug intervention is often associated with non-specific targets, to investigate the specific contribution of H1R and H2R to the pro-locomotion effect of SUB glutamatergic neurons, we infused the H1R or H2R knock-down shRNA virus into the SUB of *CaMKIIα-Cre* mice to selectively suppress H1R or H2R expression in SUB glutamatergic neurons (Fig. 6j1). In situ hybridization verified that a low mRNA expression level of H1R and H2R in SUB glutamatergic neurons respectively (Fig. 6j2). Remarkedly, our findings revealed that the pro-locomotion of Thio in SUB was abolished when H2R was knocked down in SUB glutamatergic neurons, while knockdown of H1R partially attenuated the effect of Thio in SUB (Fig. 6k, l). These data suggest the H2R in SUB glutamatergic neurons mainly

https://doi.org/10.1038/s41467-024-54347-2

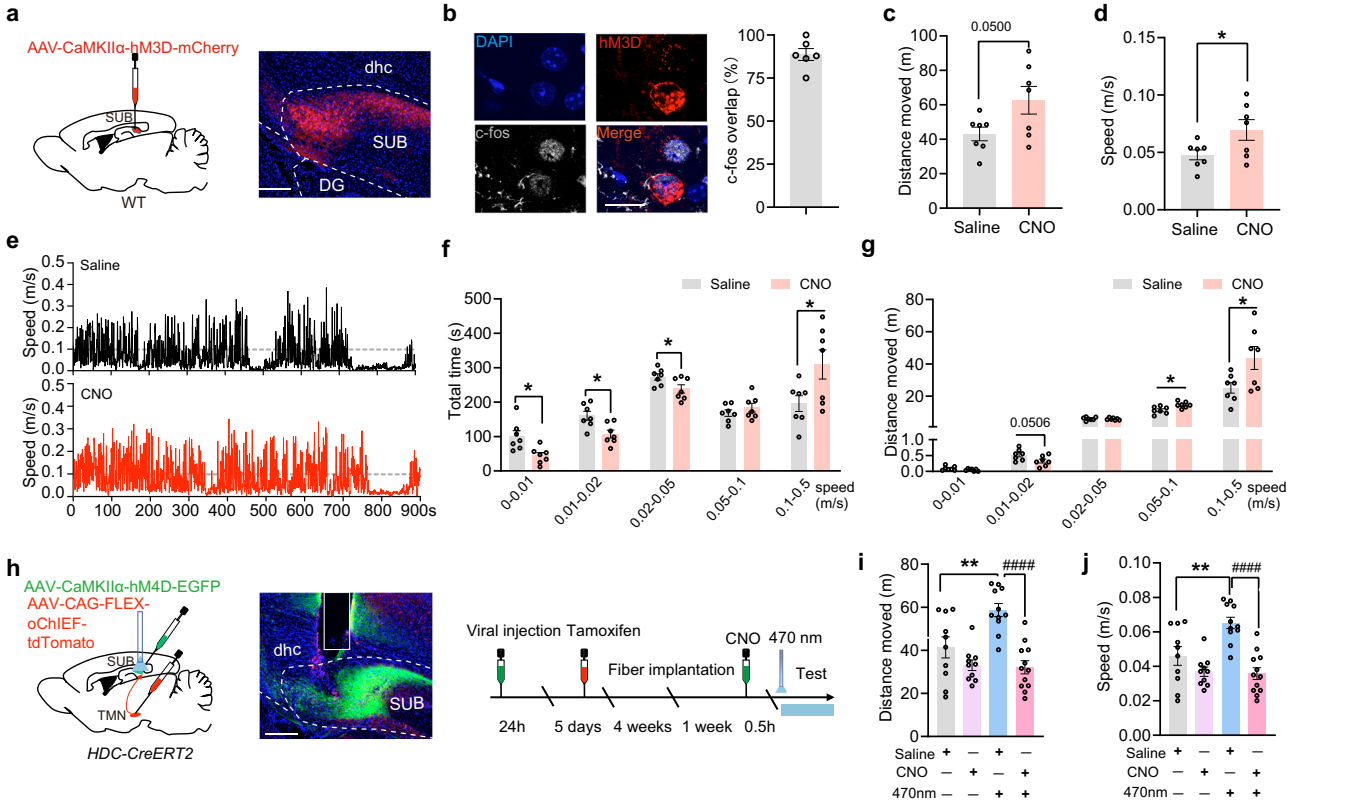

Fig. 5 | Chemogenetic inhibition of SUB glutamatergic neuron blocks pro-locomotion effect of TMN-SUB histaminergic circuit. a Schematic and image of injection of AAV-CaMKIIα-hM3D-mCherry into SUB of WT mice, scale bar = 200 μm. **b** CaMKIIα-hM3D-based glutamatergic neuron excitation in vivo resulted in c-fos expression in SUB. $n = 6$ mice. Effects of chemogenetic activation of SUB glutamatergic neurons on the distance traveled (**c**), and average speed (**d**) in open field test, $n = 7$ mice (**c**: $p = 0.05$; **d**: $^{*}p = 0.0496$). **e** Representative velocity distribution of saline control group and the CNO group. Total time (**f**), and distance moved (**g**) in open field test in 5-speed subsections of saline control group and CNO group. $n = 7$ mice (**f**: $^{*}p = 0.0100$, $^{*}p = 0.0101$, $^{*}p = 0.0381$, $p = 0.3358$, $^{*}p = 0.0362$; **g**: $p = 0.1169$, $p = 0.0506$, $p = 0.7248$, $^{*}p = 0.0116$, $^{*}p = 0.0349$). **h** Schematic diagram and representative image of viral injection of AAV-CAG-FLEX-oChIEF-tdTomato into the TMN, and AAV-CaMKIIα-hM4D-GFP into the SUB of *HDC-CreERT2* mice, and the timeline schematic diagram. scale bar = 200 μm. Effects of optogenetic activation of TMN-SUB circuit terminals combined with chemogenetic inhibition of SUB glutamatergic neurons on distance traveled (**i**), average speed (**j**) in the open field test. Saline group, $n = 10$ mice; CNO group, $n = 10$ mice; saline + 470 nm group, $n = 11$ mice; CNO + 470 nm group, $n = 12$ mice (**i**: $^{**}p = 0.0060$ saline + 470 nm vs. saline group, $^{\#\#\#\#}p < 0.0001$ CNO + 470 nm vs. saline + 470 nm group; **j**: $^{**}p = 0.0060$ saline + 470 nm vs. saline group, $^{\#\#\#\#}p < 0.0001$ CNO + 470 nm vs. saline + 470 nm group). Two-tailed Student's *t* test for (**c**, **d**, **f**, **g**) and one-way ANOVA followed by the Turkey's post hoc test for (**i**, **j**). Schematics in **a**, **h** were drew by PowerPoint. Bar graphs represent mean ± SEM. Source data are provided as a Source Data file.

mediates the pro-locomotion function of the TMN-SUB histaminergic circuit.

RSG is the downstream output of SUB glutamatergic fast locomotor cell

The SUB plays a pivotal role in encoding the animal's location, trajectory, and speed via various downstream circuits, particularly emphasizing the specialized encoding of speed information by the RSG-projecting SUB circuit[30]. We thus hypothesized that RSG may route the accelerated locomotion of the TMN-SUB histaminergic circuit. To gain deeper insights into the speed related function of the locomotion-activated neurons in SUB, we labeled these neurons by using the activity-dependent neural tagging approach with the ESARE promoter combined with chemogenetic virus and calcium activity recording virus (Fig. 7a, b). Chemogenetic activation of locomotion-activated SUB neurons increased the traveled distance and speed of mice, whereas inactivation of these neurons led to a reduction in locomotion (Fig. 7c, d). Speed subsections analysis demonstrated that chemogenetic activation of locomotion-activated SUB neurons enhanced the high-speed locomotion (Supplementary Fig. 9a, b), whereas chemogenetic inhibition of these neurons showed the opposite effect (Supplementary Fig. 9c, d), suggesting the critical role of SUB neurons in accelerated locomotion. To investigate whether chemogenetic approaches influenced the neural activity response to locomotion of these neurons, we analyzed the activity during the acceleration initiation period and found that activation of hM3D-expressed locomotion-activated SUB neurons reinstated increased activity (Fig. 7e–g), whereas inactivation of hM4D-expressed locomotion-activated SUB neurons abolished this characteristic (Fig. 7h–j). These data highlight the important role of locomotion-activated SUB neurons in regulating accelerated locomotion

To decipher the circuitry underlying the transmission of accelerated locomotion information by TMN-SUB histaminergic circuit, we performed anterograde viral tracing to label the locomotion-activated SUB neurons and observe their downstream fiber distribution (Fig. 7k). The fibers were dominantly observed in RSG, anteroventral thalamus nucleus (AV), and medial mamillary nucleus (MMB) (Fig. 7l). Next, we examined whether TMN-SUB stimulation-activated SUB neurons directly project RSG, a key brain regions involved in encoding speed information from SUB neurons[30], activity-dependent neural tagging approach was used by injection of the optogenetic activation virus AAV-CAG-FLEX-OChIEF-tdTomato into TMN, mixed combination of AAV-ESARE-ERT2-Cre-ERT2 and AAV-EF1a-DIO-EYFP into the SUB to label the TMN-SUB terminal stimulation-activated SUB neurons, combined with retrograde viral tracing by injection the AAV2/2-Retro-hSyn-

https://doi.org/10.1038/s41467-024-54347-2

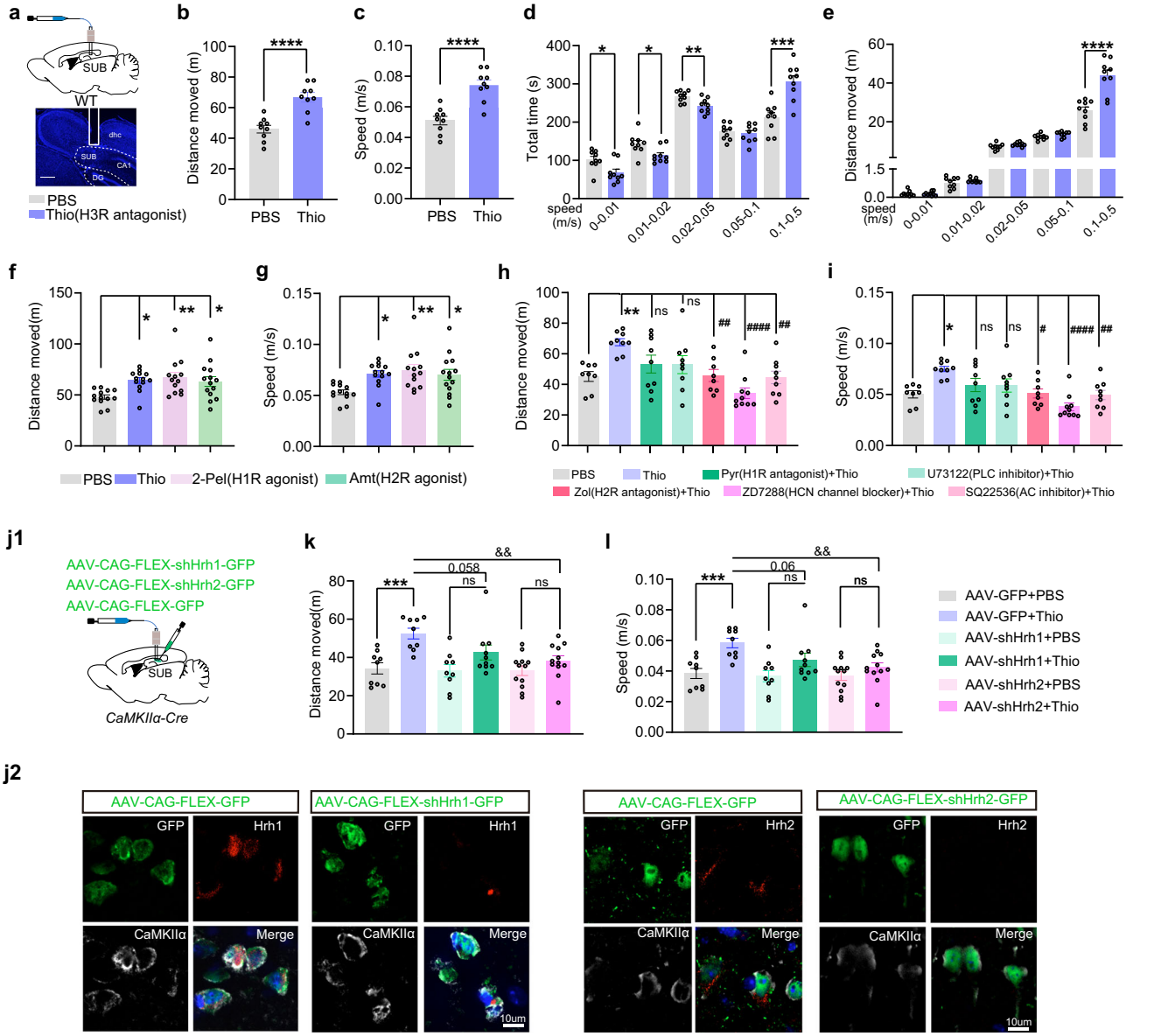

Fig. 6 | H2R in SUB glutamatergic neurons mainly mediate the pro-locomotion function of histamine-tuned circuit. a WT mice were implanted cannula in SUB, scale bar = 400 μm. Effects of administration of H3R antagonist on distance (**b**), speed (**c**) and 5-speed subsections analysis for active time (**d**), distance (**e**) in open field test. $n = 9$ mice ($^{****}p < 0.0001$ for (**b**) and (**c**); **d**: $^{*}p = 0.0154$, $^{*}p = 0.0195$, $^{**}p = 0.0073$, $p = 0.6811$, $^{***}p = 0.0003$; **e**: $p = 0.9120$, $p = 0.3507$, $p = 0.0719$, $p = 0.0535$, $^{****}p < 0.0001$). Effects of Thio and H1R/H2R-agonist on distance (**f**), speed (**g**) in open field test, $n = 13, 13, 13, 14$ mice for PBS, Thio, 2-Pel, Amt group (**f**: $^{*}p = 0.0148$, $^{**}p = 0.0028$, $^{*}p = 0.0193$; **g**: $^{*}p = 0.0141$, $^{**}p = 0.0029$, $^{*}p = 0.0201$). Effects of Thio combined with H1R/H2R-related drugs on distance (**h**), speed (**i**), $n = 8, 9, 9, 9, 8, 10, 9$ mice for PBS, Thio, Pyr + Thio, U73122 + Thio, Zol + Thio, ZD7288 + Thio, SQ22536 + Thio group (**h**: $^{**}p = 0.0035$ vs. PBS; $^{\#\#}p = 0.0049$, $^{\#\#\#\#}p < 0.0001$, $^{\#\#}p = 0.0019$ vs. Thio; **i**: $^{*}p = 0.0120$ vs. PBS; $^{\#}p = 0.0172$, $^{\#\#\#\#}p < 0.0001$, $^{\#\#}p = 0.0067$ vs. Thio), ns with respect to Thio group. **j** *CaMKIIα-Cre* were injected with knockdown virus (**j1**), validation of H1R/H2R expression with CaMKIIα immunostaining, scale bar = 10 μm (**j2**). Distance (**k**), and speed (**l**) in open field test of H1R/H2R knockdown mice, $n = 9, 9$ for AAV-GFP group; $n = 9, 10$ for AAV-shHrh1 group; $n = 12, 12$ for AAV-shHrh2 group (**k**: $^{***}p = 0.0004$ vs. PBS, $^{\&\&}p = 0.0017$ vs. AAV-GFP + Thio; **l**: $^{***}p = 0.0005$ vs. PBS, $^{\&\&}p = 0.0017$ vs. AAV-GFP + Thio). Two-tailed Student's *t* test for (**b**–**e**, **k**, **l**) and one-way ANOVA followed by post-Dunnett's test for (**f**–**i**). Schematics in **a**, **j1** were drew by PowerPoint. Bar graphs represent mean ± SEM. Source data are provided as a Source Data file.

tdTomato into RSG (Fig. 7m). Notably, TMN-SUB terminal stimulation-activated SUB neurons were partially overlapped with the RSG-retrograde labeled tdTomato (Fig. 7n, o). To functionally validate the TMN-SUB-RSG tri-synaptic connection, we injected the AAV2/2-Retro-hSyn-GCaMP6s into RSG, combined with optogenetic activation virus to label the TMN-SUB fibers (Fig. 7p). The fiber photometry data showed that the activity of RSG-projecting SUB neurons increased upon stimulation of TMN-SUB histaminergic circuit (Fig. 7q–s). These data unequivocally establish the TMN-SUB-RSG may be the circuit basis for histamine-tuned SUB circuit in controlling accelerated locomotion.

Discussion

The swift emergence of the role of TMN histaminergic neurons in locomotion has generated disparate findings in existing literature[10,13,16,17]. For example, ventral hippocampal or midbrain tectum injection of histamine inhibited locomotion[48–50], whereas dorsal hippocampal and intracerebellar histamine application showed no effect[10,49,50]. In this study, we revealed a histaminergic circuit targeting SUB in accelerated locomotion in both neutral and alert conditions (Supplementary Fig. 10).

The beginning of the research, we delineate the features of the TMN histaminergic neurons responsive solely respond to the

https://doi.org/10.1038/s41467-024-54347-2

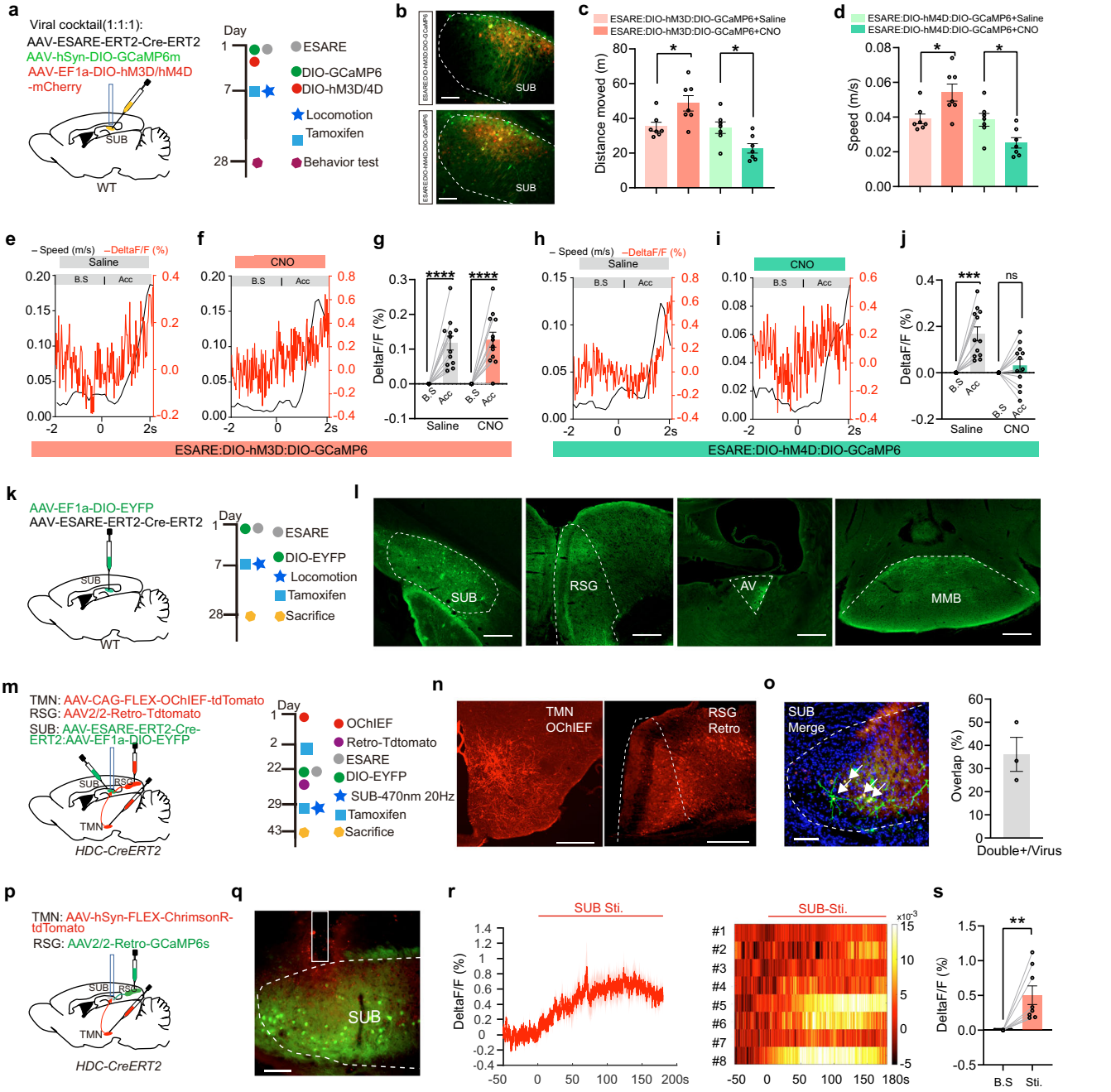

Fig. 7 | RSG is the downstream output of the TMN-SUB histaminergic circuit. **a** WT mice were injected with mixed AAV-ESARE-ERT2-Cre-ERT2, AAV-hSyn-DIO-GCaMP6m, and AAV-hSyn-DIO-hM3D(Gq)-mCherry/AAV-hSyn-DIO-hM4D(Gi)-mCherry into SUB. **b** Expression of hM3D-expressed (top) and hM4D-expressed (bottom) SUB treadmill training-labeled c-fos+ neuron, scale bar = 200 μm. Effects of chemogenetic activation or inhibition of SUB treadmill training-labeled c-fos+ neuron on total distance (**c**), speed (**d**) in open field test. $n = 7$ mice (**c**: $^{*}p = 0.0218$, $^{*}p = 0.0165$; **d**: $^{*}p = 0.0197$, $^{*}p = 0.0160$). **e**–**g** Fluorescence value with corresponding speed, and quantification (**g**) of calcium activity of hM3D-expressed SUB treadmill training-labeled c-fos+ neuron in two groups during acceleration. $n = 12$ mice ($^{****}p < 0.0001$). **h**–**j** Fluorescence value with corresponding speed, and quantification (**j**) of calcium activity of hM4D-expressed SUB treadmill training-labeled c-fos+ neuron in two groups during acceleration. $n = 12$ mice ($^{***}p = 0.0002$, $p = 0.2473$). Schematic of injection of mixed AAV-ESARE-ERT2-Cre-ERT2, AAV-EF1a-DIO-EYFP into SUB of WT mice (**k**), and expression (**l**) of SUB treadmill training-labeled c-fos+ neuron in SUB with fiber distribution in RSG, AV, MMB. Scale bar = 400 μm. **m** *HDC-CreERT2* mice were injected with AAV-CAG-FLEX-oChIEF-tdTomato into TMN, mixed AAV-ESARE-ERT2-Cre-ERT2, AAV-EF1a-DIO-EYFP into SUB to label TMN-SUB circuit-activated c-fos+ neurons combined with injection of AAV2/2Retro-hSyn-tdTomato into RSG. Viral expression in TMN and RSG, scale bar = 400 um (**n**), image and quantification (**o**) of TMN-SUB circuit-activated c-fos+ SUB neurons overlapping with Retro-tdTomato in SUB, $n = 3$ mice, scale bar = 100 μm. **p**–**s** Schematic diagram (**p**), image (**q**) of injection of AAV-hSyn-FLEX-ChrimsonR-tdTomato into TMN and AAV2/2Retro-hSyn-GCaMP6s into RSG of the *HDC-CreERT2* mice. Scale bar = 100 μm. Fluorescence values, heatmap (**r**), and quantification (**s**) of calcium activity of RSG-projecting SUB neurons during TMN-SUB circuit activation. $n = 8$ mice, $^{**}p = 0.0072$. Two-tailed Student's *t* test for (**c**, **d**, **g**, **j**, **s**). Schematics in **a**, **k**, **m**, **p** were drew by PowerPoint. Bar graphs represent mean ± SEM. Source data are provided as a Source Data file.

acceleration phase of locomotion in various locomotor tests. Notably, in the alert-escape test, the calcium activity of TMN histaminergic neurons maintained a high level even the locomotion speed has been decelerated to baseline. Functionally, optogenetic modulation of TMN histaminergic neurons had no effect on spontaneous locomotion under neutral conditions, but was both sufficient and necessary to regulate accelerated locomotion during alert-escape behavior. Taken together, these findings suggest that TMN histaminergic neurons may contribute to accelerated locomotion in general condition, but may show different features of accelerating locomotor in various situations where stress, emotion, or environmental demands fluctuate. Their activity appears to be closely tied to the behavioral context, potentially supporting a role in fine-tuning locomotor outputs and maintaining arousal levels in response to changes in stress or emotional state such as alert. This conjectures also inspired and supported by previous researches. For example, the cuneiform nucleus is considered as the primary brain area to initiate locomotion and regulate animal's locomotion speed[27], which also shows contextual dependent in regulating locomotion[51]. Therefore, this could ensure that motor responses are appropriately scaled and timed according to the specific needs of the situation, whether it be initiating movement, adjusting to ongoing changes in locomotion, or sustaining alertness during critical moments. Classical theory suggests that the motor cortex, basal ganglia brainstem, and spinal cord control animal movement, including locomotion initiation, execution, and speed, largely based on neutral or reward-based contexts[51–54]. However, movement can be triggered as the accelerated locomotion, when animal received strong external cues. The inquiry delves into the necessity of additional circuits and mechanisms for initiating behaviors in the appropriate sequence, context, and timing, along with exploring how purposeful movements can be initiated independently of explicit external triggers. Here we expanded role of histaminergic signaling in emotion-driven accelerated locomotion. Beyond its role in physical conditions, the TMN histaminergic system is linked to central nervous system disorders with movement impairments, such as Parkinson's disease, Huntington's disease, and schizophrenia[55–57]. Understanding these mechanisms is crucial for addressing neurological disorders affecting self-initiated movements and action selection, including Parkinson's disease, stroke, attention deficit and hyperactivity disorder.

Given that, EC and SUB are both brain regions distributed speed cells, while the dynamic change of histamine level during locomotion, and the function between the two histaminergic circuits are different. Notably, a pronounced elevation in histamine level aligned with the accelerated locomotion was observed specifically in the SUB. Interestingly, we found that both TMN histaminergic neuronal activity (Fig. 1e, f) and histamine release in the SUB (Fig. 2i, j) showed an increasing pattern with some detailed dynamic inconsistencies during accelerated locomotion. Two possible reasons may account for that: (1) Kinetic differences of soma and axon. Neuronal activation triggers calcium influx, leading to neurotransmitter release[58,59], indicating that neuronal activity is faster than neurotransmitter release and thus exhibits different dynamics. (2) Heterogeneous subpopulation of histaminergic neurons. Previous studies have shown that calcium activity in different downstream fibers can respond differently to the same stimuli, which also showed dynamic inconsistencies to the neuronal body activity[60]. While calcium signals in the TMN histaminergic cell body reflect overall local neuronal activity, histamine release from SUB terminals originates from only a small subset of neurons, leading to differing dynamics between neuronal body activity and terminal histamine release.

In the context of alert-escape behavior, the TMN-SUB histaminergic circuit exhibited a potent directional modulation effect on active accelerated locomotion by enhancing the max speed. These findings raise the possibility of the modulation function of histamine-tuned SUB circuits in distinct active accelerated locomotion. Conversely, optogenetic modulation of the TMN-EC histaminergic circuit had no apparent effect on locomotion. Therefore, this is one of the possibilities that supports manipulation of TMN histaminergic neurons showed no effect on spontaneous active locomotion. These results indicate the complexity of the neural circuitry of histamine modulation of locomotion, which partially explains the inconsistent results of previous nonspecific pharmacological intervention. The divergence in the observed effects could be attributed to distinct projections from various upstream TMN histaminergic neurons into SUB and EC or the potential influence of TMN histaminergic neurons on non-speed cells in EC. This interpretation aligns with the heterogeneous morphological characteristics of histaminergic neurons at the single-cell level[5]. Specifically, our investigation elucidates that the role of TMN-SUB histaminergic neural circuit in encoding accelerated motor behavior. This enhances our comprehension of neural circuits mechanisms governing accelerated locomotion. Previous studies have indirectly indicated that SUB is involved in locomotion through in vivo electrophysiological local field potentials recording[61], and c-fos staining[62]. We provided direct evidence that SUB glutamatergic "fast locomotor cells", which were finely tuned by TMN histaminergic system, could modulate spontaneous accelerated locomotion of mice. Moreover, it is worth noting that we found the TMN-SUB histaminergic circuit drives accelerated locomotion in a context-dependent manner. As shown in Fig. 2 and Supplementary Fig. 3, although histamine level was increased in both natural and alert-driven acceleration locomotion, but it was not always linear response to running speed in alert-driven accelerated locomotion. As a support, optogenetic activation of TMN-SUB circuit was sufficient to induce acceleration locomotion in various natural and alert condition. While, optogenetic inhibition of TMN-SUB circuit reduced acceleration locomotion only in alert condition. Therefore, we conclude that TMN-SUB circuit is involved in the sensory representation of speed/acceleration or the dynamics coding of speed.

The RSG, which integrates rich sensory, motor, and spatial signals from multiple brain regions (including the hippocampal system), is involved in a wide range of cognitive functions[63], and encodes the angular head velocity of mice that guarantees animals to navigate the environment[64]. Notably, RSG-projecting SUB neurons encode locomotion velocity information specifically[30]. Our study indicated that locomotion-activated SUB neurons fibers distributed in RSG, AV and MMB. Of noted, approximately 30% of RSG-projecting SUB neurons were activated during photo-stimulation of the TMN-SUB histaminergic circuit. This highlights the role of the trisynaptic TMN-SUB-RSG circuit in accelerated locomotion and provides insights into how SUB neurons process locomotion information.

Our findings also provide new insights into the action of histamine receptors in accelerated locomotion. Previous literature has presented conflicting evidence regarding the roles of H1R and H2R in mediating the effects of histamine on locomotion[49,65]. In the present study, we found that administration of the H3R antagonist in SUB enhanced the accelerated locomotion of mice into a high frequency of super high-speed movement. Specifically, accelerated locomotor-promoting effects of the TMN-SUB histaminergic circuit were found to be mediated primarily through H2R-AA and H2R-HCN pathway. This finding expands the understanding of the regulatory role of histamine receptors in the brain for accelerated locomotion. The regulation of neuronal excitation by H1R and H2R in the brain is complex and may have a coordinated mode of action[44]. Previous studies indicated that different type of receptors may form heterodimeric receptor, such as dopamine D2 receptor and H3R[66]. Thus, whether H1R and H2R form of heterodimeric receptors in the hippocampus and play similar synergistic roles deserves further validation.

In summary, this study identifies the critical role of TMN histaminergic neurons in general accelerated locomotion, especially in the alert-related emotional responses, delineating the SUB-projecting

histaminergic circuit and cellular mechanism. This provides a theoretical basis for understanding neural circuit mechanisms during alert-driven accelerated locomotion.

Methods

Animals

Male and female C57BL/6 wild-type (WT) mice and transgenic mice bred on the C57BL/6 genetic background, as well as male CD1 mice were used in this study. The WT mice and transgenic mice used in this study are 2–4 months old, and the CD1 mice are 6–8 months old. The *CaMKIIα-Cre* mice (stock number: 005359) were genotyped according to the protocols provided by Jackson Laboratory. The *HDC-CreERT2* mice were constructed by Shanghai Bio-model Organisms Science, which is tamoxifen-inducible needing an injection of tamoxifen (100 mg/kg, sigma) in consecutive 5 days to drive virus expression. We obtained *HDC-CreERT2: Ai47* mice by crossing *HDC-CerER* and *Ai47* (GFP) reporter mice. The *Ai47* reporter mice were obtained by the kind gift from Prof. Zilong Qiu (Chinese Academy of Science, Shanghai, China). All mice were housed in a 12 h light/12 h dark cycle (lights on from 8:30 to 20:30) at the temperature of 22 ± 2 °C, humidity 50 ± 10% and with ad libitum food and water. After surgery, mice were housed separately. Behavior experiments were performed in daylight (between 8:30 and 18:30). All experiments were carried out following the National Institutes of Health guidelines, and all procedures were approved by the local ethics review committee of Zhejiang Chinese Medical University.

Viral vectors

AAV-hSyn-DIO-GCaMP6m (viral titers: 1.36×10^{13} vg/mL, serotype: AAV2/9), AAV-CAG-FLEX-oChIEF-tdTomato (viral titers: 3.02×10^{12} vg/mL, serotype: AAV2/9), AAV-EF1a-DIO-EYFP (viral titers: 1.46×10^{13} vg/mL, serotype: AAV2/9), AAV/Retro-hSyn-GCaMP6s (viral titers: 2.03×10^{13} vg/mL, serotype: AAV2/2), AAV/Retro-hSyn-tdTomato (viral titers: 1.00×10^{13} vg/mL, serotype: AAV2/2), AAV-hSyn-FLEX-ChrimsonR-tdTomato (viral titers: 1.90×10^{13} vg/mL, serotype: AAV2/9), AAV-CaMKIIα-GCaMP6s (viral titers: 2.82×10^{12} vg/mL, serotype: AAV2/8), AAV-hSyn-DIO-hM4D(Gi)-mCherry (viral titers: 3.20×10^{12} vg/mL, serotype: AAV2/9), AAV-hSyn-DIO-hM3D(Gq)-mCherry (viral titers: 2.44×10^{12} vg/mL, serotype: AAV2/9), AAV-CaMKIIα-hM3D(Gq)-mCherry (viral titers: 3.00×10^{12} vg/mL, serotype: AAV2/9), and AAV-ESARE-ERT2-Cre-ERT2 (viral titers: 1.45×10^{13} vg/mL, serotype: AAV2/9) were purchased from Taitool Bioscience Co., Ltd (Shanghai, China). AAV-hSyn-FLEX-mCherry-2A-TVA-2A-RvG (viral titers: 1.73×10^{13} vg/mL, serotype: AAV2/9) and RV-EnvA-△G-EGFP (Rabie Viru, viral titers: 1.00×10^{9} IFU/mL) purchased from Taitool Bioscience Co.,Ltd were used for monosynaptic retrograde tracing. AAV-CAG-FLEX-ArchT-GFP (viral titers: 1.29×10^{13} vg/mL, serotype: AAV2/9) and AAV-CaMKIIα-hM4D(Gi)-EGFP (viral titers: 7.04×10^{12} vg/mL, serotype: AAV2/9) were purchased from OBiO Technology Co.,Ltd (Shanghai, China). Histamine H1R and H2R were knocked down by using AAV-CAG-FLEX-shHrh1-GFP (viral titers: 1.98×10^{13} vg/mL, serotype: AAV2/8) and AAV-CAG-FLEX-shHrh2-GFP (viral titers: 1.27×10^{13} vg/mL, serotype: AAV2/8), and the AAV-CAG-FLEX-GFP was used as control (viral titers: 1.14×10^{13} vg/mL, serotype: AAV2/8) purchased from OBiO Technology Co., Ltd. AAV-hSyn-HA1h (viral titers: 1.27×10^{13} vg/mL, serotype: AAV2/9) was purchased from Vigene Bioscience Co., Ltd (USA) to record the histamine concentration changes. AAV-EF1a-FLEX-taCasp3-TEVp (viral titers: 5.36×10^{12} vg/mL, serotype: AAV2/9) and AAV-CAG-DIO-mCherry (viral titers: 5.09×10^{12} vg/mL, serotype: AAV2/9) were purchased from BrainVTA Co., Ltd (Wuhan, China). All viral vectors were aliquoted and stored at −80 °C.

Viral injection and cannula/optic fiber implantation

Mice were anesthetized with sodium pentobarbital (50 mg/kg, i.p) prior to being meticulously positioned in a stereotaxic apparatus (RWD Life Science, Shenzhen, China) for subsequent stereotactic surgery. To maintain the mice's body temperature, a heating pad (RWD Life Science, Shenzhen, China) was laid on the stereotaxic apparatus. For precise calcium activity, optogenetic or chemogenetic viral delivery, the virus was injected into the TMN (0.3 μL, AP: −2.1 mm, ML: ±0.8 mm, DV: −5.5 mm), SUB (0.2 μL, AP: −3.4 mm, ML: ±2.0 mm, DV: −1.8 mm), EC (0.3 μL, AP: −4.6 mm, ML: ±3.5 mm, DV: −4.5 mm), or RSG (0.2 μL, AP: −2.7 mm, ML: −0.7 mm, DV: −1.0 mm). A 1 μL syringe (Zhenhai glass Co. LTD, Ningbo, China) connected with a glass microelectrode was controlled by an injection pump (Micro 4, World Precision Instruments, USA), ensuring a steady viral delivery at flow speed of 50 nL/min. Following the completion of viral delivery, the glass microelectrode remained in the targeted region for 10 min and then slowly withdrawn. Expression of the all the AAV virus vectors was sustained for a period of 3–4 weeks. For the calcium activity recording and optogenetics, the optic fibers (Inper, Co., Ltd, China) were implanted above the TMN, SUB, or EC. For the pharmacological intervention, the cannulas (62004, RWD Life Science, Shenzhen, China) were implanted above the SUB. Subsequent to the accomplishment of behavioral experiments, the accurate position of viral expression, cannula, and optic fiber was confirmed for further data analysis.

Fiber photometry

To record and characterize the calcium activity of TMN histaminergic neurons and SUB glutamatergic neurons, AAV-hSyn-DIO-GCaMP6m or AAV-CaMKIIα-GCaMP6s were delivered into the TMN or SUB, respectively. For monitoring the histamine concentration fluctuations, AAV-hSyn-HA1h was delivered into SUB and EC. Following the mixed AAV-ESARE-ERT2-Cre-ERT2 and AAV-hSyn-DIO-GCaMP6m or mixed AAV-ESARE-ERT2-Cre-ERT2, AAV-hSyn-DIO-GCaMP6m and AAV-hSyn-DIO-hM3D(Gq)-mCherry/AAV-hSyn-DIO-hM4D(Gi)-mCherry virus injection, an optical fiber (Inper Ltd., China) was strategically positioned above the SUB. Fiber photometry of calcium signals was performed 1 week after surgery in mice, utilizing a fiber photometry system (Inper Ltd., China). Employing the CMOS imaging technique, calcium signals were recorded. The 470 nm and 410 nm lights were alternatively given during recording, in which the 410 nm was used as the internal reference control. All the data were corrected to mitigate the impact of fluorescence attenuation during long-term exposure recording. The baseline average fluorescence change was denoted as $F0$. Specific events-induced fluorescence change of was quantified as ($\Delta F/F0$) by calculating $((F-F0)/F0)$. Data were analyzed by Inper plot (Inper Ltd., China). For Fig. 4e–h and Supplementary Fig. 4a–d, the photostimulation was given by a 635 nm red light and that will not be detected by the fiber photometry system. The relevant data were represented as average linear fluorescence change, heatmap, and statistical graphs.

Optogenetic manipulations

Blue light (470 nm) or yellow light (589 nm) was delivered into the targeted brain region via a 200 μm diameter optic fiber (Inper, Co., Ltd, China). During the experiments, the photo laser stimulator (Inper, Co., Ltd, China) was triggered with a remote controller. Optogenetic activation or inhibition was achieved using the 470 nm blue light (20 Hz, 5 mW, 10 ms/pulse) or 589 nm yellow light (continuous, 5 mW) respectively. For validation of functional connectivity, 635 nm red light (20 Hz, 5 mW, 10 ms/pulse) was delivered into the SUB. The intensity of light was measured by an optical power meter (THORLABS, USA).

Chemogenetic manipulations

To unravel the role of SUB glutamatergic neurons in the TMN-SUB histaminergic circuit, mice were intraperitoneally injected with clozapine-N-oxide (CNO, 1 mg/kg, ab141704, Abcam, UK) dissolved in

the 0.9% saline. The injection was administered 30 min prior to the commencement of behavioral tests.

Pharmacological interventions

To assess the effect of histamine in the SUB and the related receptor actions, the H3R antagonist (Thioperamide maleate, 10 μg/site, 0.5 μL, ab120021, Abcam, UK), and H1R agonist (2-(2-pyridyl)-ethylamine, 10 μg/site, 0.5 μL, A55306, Sigma, USA), H2R agonist (Amthamine, 10 μg/site, 0.5 μL, A4730, Sigma, USA), were microinjected into the SUB. To further investigate the postsynaptic receptor mechanism of the pharmacological action of thioperamide, we combined the H1R antagonist (Pyrilamine, 10 μg/site, 0.5 μL, P5514, Sigma, USA) and H2R antagonist (Zolantidine, 10 μg/site, 0.5 μL, 1070, Tocris, USA), and the H2R downstream HCN channel blocker (ZD7288, 10 μg/site, ab147489, Abcam, UK), and Adenine cyclase inhibitor (SQ 22536, 10 μg/site, ab120642, Abcam, UK), as well as the inhibitor of H1R-coupled Phospholipase C, PLC (U-73122, 10 μg/site, 0.5 μL, U6765, Sigma, USA). All the reagents were dissolved in PBS and stored at −20 °C before use.

Monosynaptic retrograde tracing

The AAV-hSyn-FLEX-mCherry-2A-TVA-2A-RvG (0.2 μL) was delivered into the SUB of the *CaMKIIα-Cre* mice. Following a period of 3 weeks to allow for optimal viral expression, a reconstructive rabies virus, RV-EnvA-△G-EGFP (0.08 μL) was delivered into the SUB. The rabies virus, engineered for retrograde transport could reach to the neuronal axon and infect the presynaptic neurons.

Activity-dependent neuronal labeling

For identification of neurons activated during optogenetic stimulation of the TMN-SUB histaminergic circuit, AAV-CAG-FLEX-oChIEF-tdTomato was delivered into TMN. Subsequent to 3 weeks of expression, a 1:1 mixed combination of AAV-ESARE-ERT2-Cre-ERT2 and AAV-EF1a-DIO-EYFP was injected into the SUB of the *HDC-CreERT2* mice. An intraperitoneal injection of tamoxifen (200 mg/kg; Sigma-Aldrich) was administrated 2 h prior to photo-stimulation of SUB (470 nm, 20 Hz, 5 mW, 10 ms/pulse, 30 s ON and 30 s OFF, 30 min). Tamoxifen, dissolved in the corn oil (20 mg/mL), was prepared in the water bath at 40 °C.

To label neurons activated during treadmill locomotion which could be simultaneously manipulate and record neural activity, a 1:1:1 mixed AAV-ESARE-ERT2-Cre-ERT2, AAV-hSyn-DIO-GCaMP6m, and AAV-hSyn-DIO-hM3D(Gq)-mCherry (or AAV-hSyn-DIO-hM4D(Gi)-mCherry) was injected into the SUB with a total volume of 0.2 μL in the WT mice. The tamoxifen was intraperitoneally injected 2 h before treadmill training. The mice were subjected to high-speed treadmill training (10 m/min, 15 s ON, 5 s OFF, 1 min/cycle, total of 6 cycles). To minimize the non-specific neuronal labeling due to environmental background noise, the mice were housed in their home cages in the quiet room for 8 h before and after tamoxifen administration.

Behavioral tests

Before the tests, a period of 3–5 days was dedicated to acclimating all mice to the experimenters to mitigate the undesired anxiety and stress. All the behavioral tests were orchestrated during daylight (between 8:30 and 18:30). On the day of testing, mice were placed into the testing room no less than 30 min before tasks. Behavioral testing and data analysis were performed in a double-blind manner, ensuring the testers remained unaware of the grouping information pertaining to the experimental mice during data analysis. A minimum interval of 5 days was allowed between each behavioral test to afford the mice sufficient rest and recovery.

Spontaneous locomotion test

The spontaneous locomotion activity of mice was evaluated in the open field test in an acrylic chamber devoid of a roof (45 × 45 × 45 cm). Mice were granted a 15 min period to freely explore the chamber with the center zone accounting for 25% of the total area. The number of feces produced by each mouse was recorded. After testing, the chamber was cleaned with 75% ethanol after each test session, and the next mouse was placed into the chamber after full volatilization. A total of 15 min test was recorded by ANYMAZE software (ANY maze Video Tracking System, Version 7.02, Stoelting Co., USA). For the fiber photometry data analysis, the onset of acceleration initiation was defined as events where mice speed greater than 0.06 m/s within 2 s[53,67].

Rotarod test

The rotarod test was employed to investigate the change in neuronal calcium activity and the histamine concentration during the motor coordinating process. The rotarod apparatus (LE8205, Panlab S.L.U, Spain) featured 5 compartments, each with dimensions of 6 cm in width, 3 cm in diameter, and 35 cm in height. The initial speed of the apparatus was set at 5 rpm/min and gradually accelerated to 40 rpm/min within 5 min. At the beginning of the experiment, the baseline of 1 min was recorded, followed by the calcium activity of the mice in the rotating up to 8 rpm/min, and the whole experiment was captured by the camera in real-time.

Treadmill test

The treadmill test was used to record changes in the calcium activity of neurons in target brain regions during acceleration or deceleration by setting the speed of the treadmill (ZS-PT-III, Zhongshi, China) to low speed (1 m/min, 10 s), acceleration (1–5 m/min, within 10 s), high speed (5 m/min, 10 s), deceleration (5–1 m m/min, within 10 s) and low speed (1 m/min, 10 s) for a total of 50 s in 5 consecutive phases of the exercise. Mice were placed on the treadmill to learn 5 rounds of running exercises before recording. In the formal experiment, we recorded a 1 min baseline at first, followed by calcium activity recording, and the camera was synchronized to record the whole experimental process. The treadmill was cleaned with 75% alcohol at the end of each mouse's test. For the c-fos staining, mice were placed on the treadmill for each round of running training at a high speed of 1 min (10 m/min, 15 s on, 5 s off), and the mice rested for 5 min after each round. Mice were sacrificed 90 min after 6 rounds of running training.

Novel object approaching test

The novel object approaching test was conducted by using an object with no irritating odor. The novel object utilized in this study comprised a 50 mL centrifuge tube cap affixed to the extremity of a petite wooden rod using double-sided tape. At the beginning of the experiment, a baseline was recorded for 5 min, and then the experimenter placed the centrifuge tube cap in the experimental chamber for 5 s and withdrew it after 1 min repeated the above procedure. Each mouse underwent 3 exposures to the novel object, with the entire experiment meticulously documented by the synchronized recording of the camera.

Social attack-escape test

The social attack-escape test was conducted by using unfamiliar aggressive male CD1 mice. Male mice were placed in a chamber (40 × 30 × 20 cm) lined with clean corn cob bedding for 30 min before the start of the social attack-escape experiment. An aggressive male CD1 mouse was used as the "intruder". The social attack-induced escape speed and movement distance was recorded for two consecutive light-ON/OFF cycle totaling 20 min. Escape speed was quantified as the speed of mice rapidly escaping from the CD1 mice approaching and sniffing within 10 s. The experiments were recorded and analyzed by ANYMAZE software (ANY maze Video Tracking System, Version 7.02, Stoelting Co., USA). Following each mouse test, the bedding was replaced, and the experimental chamber was wiped with 75% alcohol before introducing a new set of mice.

Immunohistochemistry and imaging

After all behavioral studies, mice were deeply anesthetized. Then, the thoracic cavity was opened to fully expose the heart, PBS was perfused via the left ventricle until the mice's viscera and mouth and nose turned white, then 4% paraformaldehyde (PFA, 4 °C) was slowly perfused until mice limbs twitch. The mouse brain was removed and fixed in 4% PFA overnight at 4 °C, and the next day the liquid was replaced with 30% sucrose solution at 4 °C for dehydration. Brain slices at a thickness of 30 μm in the coronal section were gained by a frozen slicer (NX70, Thermo Fisher, USA). Brain slices were washed with PBS to remove the OCT, and then the blocking solution (PBS solution containing 0.3% Triton X-100, 3% bovine protein serum, and 5% donkey serum) was added and blocked for 2 h at room temperature. Next, the primary antibody including rabbit anti-HDC (1:300, 03-16045, American Research, USA), rabbit anti-CaMKIIα (1:300, Ab52476, Abcam, UK), mouse anti-c-Fos (1:500, Ab208942, Abcam, UK), rabbit anti-GABA (1:200, A2052, Sigma, USA), was diluted in the blocking solution, and 300 μL of the primary antibody was added to each slice, and incubated overnight at 4 °C. The next day, PBS was added 4 times for 10 min each time at room temperature, then the secondary antibodies including, donkey anti-mouse 488 (1:500, Ab150073, Abcam, UK), donkey anti-rabbit 594 (1:500, Ab150064, Abcam, UK), and donkey anti-rabbit 647 (1:500, Ab150075, Abcam, UK), prepared by PBS was added and incubated for 2 h at room temperature to avoid light. Then, brain slices were washed with PBS for 10 min each time, 4 times. Finally, the brain slices were sealed with an anti-fluorescence cancellation containing DAPI (D12111201, Yeasen Biotech Co., Ltd., China). The slices were scanned and photographed with an automatic slide scanning microscope (DM6B, Leica, Germany).

In situ hybridization

Brain slices were cut at a thickness of 12 μm in the coronal section. In situ hybridization was performed using the RNAscope® Multichannel II Fluorescence Kit (323110, ACD, USA). First, PBS washed away the OCT on the brain slices. Then slices were soaked in the solution containing methanol and 30% hydrogen peroxide for 10 min at room temperature, and removed in 95% ethanol at room temperature for 3 min. Next, protease III is added to brain slices in a hybridization oven at 40 °C for 30 min. Hrh1 (491141, ACD, USA) or Hrh2 (517751, ACD, USA) probes were added to the slices, 5 μL per brain slice, at 40 °C for 120 min. Amplification: 5 μL AMP① was added to each brain slice at 40 °C for 30 min; 5 μL AMP② was added to each brain slice at 40 °C for 30 min; 5 μL of AMP③ was added to each brain slice at 40 °C for 15 min. Then, HRP C1 was added to the brain slice at 40 °C for 15 min, and opal 570 dye was added brain at 40 °C for 30 min. Next, HRP Blocker was added to the brain slice at 40 °C for 15 min. Then all the procedures were performed the same as immunohistochemistry.

Data analysis and statistics

All experimental tests and data analysis in this study was performed in a double-blind manner. All data were expressed as mean ± standard error (mean ± SEM). Statistical analysis was performed using Graphpad Prism software (version 9) and SPSS (version 22), and Adobe Illustrator (version 2019) was used for graphing. Data conforming to a normal distribution were compared between multiple groups using one-way analysis of variance (ANOVA) post hoc Turkey's test or Dunnett's test or Two-way ANOVA. Data with a normal distribution were analyzed between two groups using paired or unpaired with two-tailed Student's *t* test analysis. For data were not distributed normally, which were analyzed by Kruskal–Wallis test. A two-tailed $p < 0.05$ indicates a statistical difference.

Reporting summary

Further information on research design is available in the Nature Portfolio Reporting Summary linked to this article.

Data availability

All data analyzed in this research are included in this published paper and its Supplementary Information/Source data file. Any additional information related with this paper is available from the corresponding author. Source data are provided with this paper.

References

1. Svensson, E., Williams, M. J. & Schiöth, H. B. Neural cotransmission in spinal circuits governing locomotion. *Trends Neurosci.* **41**, 540–550 (2018).
2. Ferreira-Pinto, M. J., Ruder, L., Capelli, P. & Arber, S. Connecting circuits for supraspinal control of locomotion. *Neuron* **100**, 361–374 (2018).
3. Railo, H., Kraufvelin, N., Santalahti, J. & Laine, T. Rapid withdrawal from a threatening animal is movement-specific and mediated by reflex-like neural processing. *Neuroimage* **283**, 120441 (2023).
4. Leiras, R., Cregg, J. M. & Kiehn, O. Brainstem circuits for locomotion. *Annu. Rev. Neurosci.* **45**, 63–85 (2022).
5. Lin, W. et al. Whole-brain mapping of histaminergic projections in mouse brain. *Proc. Natl Acad. Sci. USA* **120**, e2216231120 (2023).
6. Arrigoni, E. & Fuller, P. M. The role of the central histaminergic system in behavioral state control. *Curr. Top. Behav. Neurosci.* **59**, 447–468 (2022).
7. Yu, X. et al. Wakefulness is governed by GABA and histamine cotransmission. *Neuron* **87**, 164–178 (2015).
8. Xu, L. et al. An H2R-dependent medial septum histaminergic circuit mediates feeding behavior. *Curr. Biol.* **32**, 1937–1948.e1935 (2022).
9. Li, B. et al. Histamine increases neuronal excitability and sensitivity of the lateral vestibular nucleus and promotes motor behaviors via HCN channel coupled to H2 receptor. *Front. Cell Neurosci.* **10**, 300 (2016).
10. Guilherme, E. M. et al. Intracerebellar microinjection of histaminergic compounds on locomotor and exploratory behaviors in mice. *Neurosci. Lett.* **687**, 10–15 (2018).
11. Mochizuki, T. Histamine as an alert signal in the brain. *Curr. Top. Behav. Neurosci.* **59**, 413–425 (2022).
12. Dong, H. et al. Genetically encoded sensors for measuring histamine release both in vitro and in vivo. *Neuron*. https://doi.org/10.1016/j.neuron.2023.02.024 (2023).
13. Imaizumi, M., Miyazaki, S. & Onodera, K. Effects of betahistine, a histamine H1 agonist and H3 antagonist, in a light/dark test in mice. *Methods Find. Exp. Clin. Pharm.* **18**, 19–24 (1996).
14. Kalivas, P. W. Histamine-induced arousal in the conscious and pentobarbital-pretreated rat. *J. Pharm. Exp. Ther.* **222**, 37–42 (1982).
15. Socha, R., Kodrík, D. & Zemek, R. Stimulatory effects of bioamines norepinephrine and dopamine on locomotion of Pyrrhocoris apterus (L.): is the adipokinetic hormone involved? *Comp. Biochem. Physiol. B Biochem. Mol. Biol.* **151**, 305–310 (2008).
16. Taylor, J. C. et al. A novel zebrafish-based model of nociception. *Physiol. Behav.* **174**, 83–88 (2017).
17. Chiavegatto, S., Nasello, A. G. & Bernardi, M. M. Histamine and spontaneous motor activity: biphasic changes, receptors involved and participation of the striatal dopamine system. *Life Sci.* **62**, 1875–1888 (1998).
18. Greenberg, M. E. & Ziff, E. B. Stimulation of 3T3 cells induces transcription of the c-fos proto-oncogene. *Nature* **311**, 433–438 (1984).
19. Severi, K. E., Böhm, U. L. & Wyart, C. Investigation of hindbrain activity during active locomotion reveals inhibitory neurons involved in sensorimotor processing. *Sci. Rep.* **8**, 13615 (2018).
20. Sternberg, J. R. et al. Optimization of a neurotoxin to investigate the contribution of excitatory interneurons to speed modulation in vivo. *Curr. Biol.* **26**, 2319–2328 (2016).

21. Wilson, R. S., Pavlic, T. P., Wheatley, R., Niehaus, A. C. & Levy, O. Modeling escape success in terrestrial predator-prey interactions. *Integr. Comp. Biol.* **60**, 497–508 (2020).
22. Lever, C., Burton, S. & O'Keefe, J. Rearing on hind legs, environmental novelty, and the hippocampal formation. *Rev. Neurosci.* **17**, 111–133 (2006).
23. Sturman, O., Germain, P. L. & Bohacek, J. Exploratory rearing: a context- and stress-sensitive behavior recorded in the open-field test. *Stress* **21**, 443–452 (2018).
24. Tan, N. et al. Lateral hypothalamus calcium/calmodulin-dependent protein kinase II α neurons encode novelty-seeking signals to promote predatory eating. *Research* **2022**, 9802382 (2022).
25. Krsiak, M. Effects of drugs on behaviour of aggressive mice. *Br. J. Pharm.* **65**, 525–533 (1979).
26. Yilmaz, M. & Meister, M. Rapid innate defensive responses of mice to looming visual stimuli. *Curr. Biol.* **23**, 2011–2015 (2013).
27. Grillner, S. & El Manira, A. Current principles of motor control, with special reference to vertebrate locomotion. *Physiol. Rev.* **100**, 271–320 (2020).
28. Sheeran, W. M. & Ahmed, O. J. The neural circuitry supporting successful spatial navigation despite variable movement speeds. *Neurosci. Biobehav. Rev.* **108**, 821–833 (2020).
29. Kropff, E., Carmichael, J. E., Moser, M. B. & Moser, E. I. Speed cells in the medial entorhinal cortex. *Nature* **523**, 419–424 (2015).
30. Kitanishi, T., Umaba, R. & Mizuseki, K. Robust information routing by dorsal subiculum neurons. *Sci. Adv.* **7**, https://doi.org/10.1126/sciadv.abf1913 (2021).
31. Spalla, D., Treves, A. & Boccara, C. N. Angular and linear speed cells in the parahippocampal circuits. *Nat. Commun.* **13**, 1907 (2022).
32. Gerlei, K. Z., Brown, C. M., Sürmeli, G. & Nolan, M. F. Deep entorhinal cortex: from circuit organization to spatial cognition and memory. *Trends Neurosci.* **44**, 876–887 (2021).
33. Issa, J. B., Radvansky, B. A., Xuan, F. & Dombeck, D. A. Lateral entorhinal cortex subpopulations represent experiential epochs surrounding reward. *Nat. Neurosci.* **27**, 536–546 (2024).
34. Tukker, J. J. et al. Microcircuits for spatial coding in the medial entorhinal cortex. *Physiol. Rev.* **102**, 653–688 (2022).
35. Heys, J. G. & Dombeck, D. A. Evidence for a subcircuit in medial entorhinal cortex representing elapsed time during immobility. *Nat. Neurosci.* **21**, 1574–1582 (2018).
36. Amalyan, S. et al. Enhanced motor cortex output and disinhibition in asymptomatic female mice with C9orf72 genetic expansion. *Cell Rep.* **40**, 111043 (2022).
37. Yao, Z. et al. A taxonomy of transcriptomic cell types across the isocortex and hippocampal formation. *Cell* **184**, 3222–3241.e3226 (2021).
38. Pelkey, K. A. et al. Hippocampal GABAergic inhibitory interneurons. *Physiol. Rev.* **97**, 1619–1747 (2017).
39. Cembrowski, M. S. & Spruston, N. Heterogeneity within classical cell types is the rule: lessons from hippocampal pyramidal neurons. *Nat. Rev. Neurosci.* **20**, 193–204 (2019).
40. Kawashima, T. et al. Functional labeling of neurons and their projections using the synthetic activity-dependent promoter E-SARE. *Nat. Methods* **10**, 889–895 (2013).
41. Lai, N. et al. Interictal-period-activated neuronal ensemble in piriform cortex retards further seizure development. *Cell Rep.* **41**, 111798 (2022).
42. Andersson, R., Galter, D., Papadia, D. & Fisahn, A. Histamine induces KCNQ channel-dependent gamma oscillations in rat hippocampus via activation of the H1 receptor. *Neuropharmacology* **118**, 13–25 (2017).
43. Terao, A., Steininger, T. L., Morairty, S. R. & Kilduff, T. S. Age-related changes in histamine receptor mRNA levels in the mouse brain. *Neurosci. Lett.* **355**, 81–84 (2004).
44. Yang, L., Wang, Y. & Chen, Z. Central histaminergic signalling, neural excitability and epilepsy. *Br. J. Pharm.* **179**, 3–22 (2022).
45. Schneider, E. H. & Seifert, R. The histamine H4-receptor and the central and peripheral nervous system: a critical analysis of the literature. *Neuropharmacology* **106**, 116–128 (2016).
46. Gao, M., Ooms, J. F., Leurs, R. & Vischer, H. F. Histamine H(3) receptor isoforms: insights from alternative splicing to functional complexity. *Biomolecules* **14**, https://doi.org/10.3390/biom14070761 (2024).
47. Panula, P. et al. International Union of Basic and Clinical Pharmacology. XCVIII. Histamine receptors. *Pharm. Rev.* **67**, 601–655 (2015).
48. Alvarez, E. O. & Guerra, F. A. Effects of histamine microinjections into the hippocampus on open-field behavior in rats. *Physiol. Behav.* **28**, 1035–1040 (1982).
49. Alvarez, E. O. & Banzán, A. M. Histamine in dorsal and ventral hippocampus. II. Effects of H1 and H2 histamine antagonists on exploratory behavior in male rats. *Physiol. Behav.* **37**, 39–45 (1986).
50. Santos, N. R., Huston, J. P. & Brandão, M. L. Escape behavior under tonic inhibitory control of histamine H(2)-receptor mediated mechanisms in the midbrain tectum. *Behav. Brain Res.* **124**, 167–175 (2001).
51. Caggiano, V. et al. Midbrain circuits that set locomotor speed and gait selection. *Nature* **553**, 455–460 (2018).
52. van der Zouwen, C. I. et al. Freely behaving mice can brake and turn during optogenetic stimulation of the mesencephalic locomotor region. *Front. Neural Circuits* **15**, 639900 (2021).
53. Capelli, P., Pivetta, C., Soledad Esposito, M. & Arber, S. Locomotor speed control circuits in the caudal brainstem. *Nature* **551**, 373–377 (2017).
54. Klaus, A., Alves da Silva, J. & Costa, R. M. What, if, and when to move: basal ganglia circuits and self-paced action initiation. *Annu. Rev. Neurosci.* **42**, 459–483 (2019).
55. Peng, J. Y. et al. Ameliorating parkinsonian motor dysfunction by targeting histamine receptors in entopeduncular nucleus-thalamus circuitry. *Proc. Natl Acad. Sci. USA* **120**, e2216247120 (2023).
56. Ma, Q. et al. Histamine H(2) receptor deficit in glutamatergic neurons contributes to the pathogenesis of schizophrenia. *Proc. Natl Acad. Sci. USA* **120**, e2207003120 (2023).
57. Martínez-Gopar, P. E. et al. Mast cells and histamine are involved in the neuronal damage observed in a quinolinic acid-induced model of Huntington's disease. *J. Neurochem.* **160**, 256–270 (2022).
58. Chen, T. W. et al. Ultrasensitive fluorescent proteins for imaging neuronal activity. *Nature* **499**, 295–300 (2013).
59. Tikkanen, T., Raatikainen, O. & Tuomisto, L. Calcium-dependent histidine and histamine release from superfused synaptosomes. *Agents Actions* **30**, 220–222 (1990).
60. Cheng, H. et al. Projection-defined median raphe Pet(+) subpopulations are diversely implicated in seizure. *Neurobiol. Dis.* **189**, 106358 (2023).
61. Trimper, J. B., Galloway, C. R., Jones, A. C., Mandi, K. & Manns, J. R. Gamma oscillations in rat hippocampal subregions dentate gyrus, CA3, CA1, and subiculum underlie associative memory encoding. *Cell Rep.* **21**, 2419–2432 (2017).
62. Gao, T. H. et al. Chronic lithium exposure attenuates ketamine-induced mania-like behavior and c-Fos expression in the forebrain of mice. *Pharm. Biochem. Behav.* **202**, 173108 (2021).
63. Mao, D., Molina, L. A., Bonin, V. & McNaughton, B. L. Vision and locomotion combine to drive path integration sequences in mouse retrosplenial cortex. *Curr. Biol.* **30**, 1680–1688.e1684 (2020).
64. Keshavarzi, S. et al. Multisensory coding of angular head velocity in the retrosplenial cortex. *Neuron* **110**, 532–543.e539 (2022).
65. Jośko, J. et al. Ontogenetic serotoninergic lesioning alters histaminergic activity in rats in adulthood. *Neurotox. Res.* **20**, 103–108 (2011).
66. Ferrada, C. et al. Interactions between histamine H3 and dopamine D2 receptors and the implications for striatal function. *Neuropharmacology* **55**, 190–197 (2008).

67. Sharma, S. et al. Inhibitory medial zona incerta pathway drives exploratory behavior by inhibiting glutamatergic cuneiform neurons. *Nat. Commun.* **15**, 1160 (2024).

Acknowledgements

This project was supported by grants from the National Key R&D Program of China (2021ZD0202803 to Z.C.), the National Natural Science Foundation of China (U21A20418 to Z.C., U23A20533 and 82373859 to Y.W., 32400832 to L.Y.), the China Postdoctoral Science Foundation (2023M743145 to L.Y.), and Research Project of Zhejiang Chinese Medical University (2023RCZXZK45 to L.Y.).

Author contributions

L.Y., Y.W., and Z.C. contributed to the conception and design of the study. L.Y., M.D.Z., Y.Z., D.X.J., L.L.Y., L.Y.X., F.F., W.K.L., Y.R.Z., and J.N.W. contributed to the acquisition and analysis of data; L.Y., Y.W., and Z.C. contributed to drafting the text and preparing the figures.

Competing interests

The authors declare no competing interests.

Additional information

Supplementary information The online version contains supplementary material available at https://doi.org/10.1038/s41467-024-54347-2.

Correspondence and requests for materials should be addressed to Yi Wang or Zhong Chen.

Peer review information *Nature Communications* thanks the anonymous reviewer(s) for their contribution to the peer review of this work. A peer review file is available.